ABSTRACT

Title of dissertation: MATHEMATICAL MODELS OF UNDERLYING DYNAMICS IN ACUTE AND CHRONIC IMMUNOLOGY

Asia Alexandria Wyatt
Doctor of Philosophy, 2019

Dissertation directed by: Professor Doron Levy
Department of Mathematics

During an immune response, it is understood that there are key differences between the cells and cytokines that are present in a primary response versus those present in subsequent responses. Specifically, after a primary response, memory cells are present and drive the clearance of antigen in these later immune responses. When comparing acute infections to chronic infections, there are also differences in the dynamics of the immune system. In this dissertation, we develop three mathematical models to explore these differences in the immune response to acute and chronic infections through the creation, activation, regulation, and long term maintenance of T cells. We mimic this biological behavior through the use of delayed differential equation (DDE) models.

The first model explores the dynamics of adaptive immunity in primary and secondary responses to acute infections. It is shown that while we observe similar amounts of antigen stimulation from both immune responses, with the incorporation of memory T cells, we see an increase in both the amount of effector T cells present

and the speed of activation of the immune system in the secondary response. We conclude that our model is robust and can be applied to study different types of antigen from viral to bacterial.

Extending our work to chronic infections, we develop our second and third models to explore breast cancer dormancy and T cell exhaustion. For our breast cancer dormancy model, we find that our model behaves similar to acute infections, but with constant antigen stimulation. Moreover, we observe the importance of immune protection on the long term survival of breast cancer cells.

In our third model we find that while memory T cells play a major role in the effectiveness of the immune system in acute infection, in chronic infections, over long periods of time, T cell exhaustion prevents proper immune function and clearance of antigen. We also observe how the lack of long term maintenance of memory T cells plays an important role in the final outcome of the system. Finally, we propose two potential extensions to the three models developed: creating a simplified acute infection model and creating a combined breast cancer dormancy model with T cell exhaustion.

MATHEMATICAL MODELS OF UNDERLYING DYNAMICS IN ACUTE AND CHRONIC IMMUNOLOGY

by

Asia Alexandria Wyatt

Dissertation submitted to the Faculty of the Graduate School of the
University of Maryland, College Park in partial fulfillment
of the requirements for the degree of
Doctor of Philosophy
2019

Advisory Committee:
Professor Doron Levy, Chair/Advisor
Professor Radu Balan
Professor Maria Cameron
Professor Pierre-Emmanuel Jabin
Professor William Fagan, Dean's Representative

Dedication

This thesis is dedicated to my mother, Altheria Wyatt, who's love and support guided me to always reach for my dreams and who's illness, rheumatoid arthritis, pushed me to study immunology. It is also dedicated to my father, Lee Wyatt, who never let me be less than who I was always meant to be and challenged me to be stronger, greater, and unmoving. I love you both.

Acknowledgments

I am eternally grateful to the people who helped to make this thesis happen. First, I would like to thank my advisor, Doron Levy, who without, none of this would be possible. It has not been an easy journey, but you stayed dedicated, patient, and a never-moving fixture along the way, and I am forever grateful!

I thank my research group, Cara, Sid, and Jesse. You all became my research family; thank you for making research a bit easier. I would also like to thank my collaborator, Grégoire Altan-Bonnet, and my committee members for helping complete this work and providing excellent feedback.

A major thank you to my family, particularly my siblings, Anatoshia, LeMona, and Adrian. We are the same brand of crazy and that's what makes us special! Thanks for always grounding me. And, a special shoutout to Mona for all of the late night, 4-hour phone calls and stopping me from walking off 'Into the Wild.'

I have many friends to thank, but to name a few, I would like to thank William (my hometown clutch), Amanda (my tall, brilliant sister), Myryah (my spicy, ride-or-die), (the friend group) Kiara, Bart, Alexa, and Lakiem, (my sister-friends) MK and Ama, and my entire DMV dance family. You all held me down throughout this process, and whether new or old, I am honored to call you my friends.

Finally, I would like to thank my heart, my person, my fiancé, Chae Clark. I could have never done this without you; you lived day to day through both the tears and the laughs. I am more than excited to live each day in gratitude for your consistent patience and love.

Table of Contents

List of Tables

List of Figures

List of Abbreviations

ACF	Asymmetric Cell-fate Model
APCs	Antigen Presenting Cells
BCCs	Breast Cancer Cells
BCR	B Cell Receptor
CM	Central Memory T Cells
CTLs	Cytotoxic T Cells
DDE	Delayed Differential Equation
DTCs	Disseminated Tumor Cells
EM	Effector Memory T Cells
IL-2	Interleukin-2
MHC	Major Histocompatibility Complex
MSCs	Mesenchymal Stem Cells
NCI	National Cancer Institute
NIH	National Institutes of Health
ODE	Ordinary Differential Equation
PD-1	Programmed Cell-death Protein 1
PDE	Partial Differential Equation
TCR	T Cell Receptor
Ths	Helper T Cells
TNF	Tumor Necrosis Factor
Tregs	Regulatory T Cells

Chapter 1: Introduction

The goal of this dissertation is to develop mathematical models to study T cell driven adaptive immunity in acute and chronic infections.

1.1 Introduction to Adaptive Immunity

The immune system fights organisms and substances that invade the body [1]. The immune system is composed of two main components: the innate immune system and the adaptive immune system. The innate immune system is the body's first line defense, incorporating factors such as anatomical barriers, natural killer cells, and antigen presenting cells (APCs), e.g., dendritic cells and macrophages. While the innate immune system provides a rapid response, these cells are neither antigen specific nor long lasting in the body. Conversely, the adaptive immune system, which includes B cells and T cells, may have a slower response to antigen stimulation, yet adaptive cells are antigen specific and can remain in the body for long periods of time. For the purposes of this study, we aim to focus on T cell driven adaptive immunity.

T cell driven adaptive immunity can be divided into three stages: activation, effector, and contraction. The activation of T cells comes as a consequence of im-

mature APCs, including both innate immune system cells and B cells, encountering antigen and undergoing a maturation process. Subsequently, these mature APCs have the ability to present antigen molecules on their cell surface to naïve effector T cells. Once APCs bind with T cells that are specific to the antigen presented, these naïve cells undergo a minimal developmental program in which they proliferate multiple times until they reach maturation. Once matured, these effector T cells are ready to perform their individual effector functions.

The role of T cells in the effector stage depends on the type of T cell, the main two being CD8+ and CD4+ T cells. The primary role for CD8+ T cells, or cytotoxic T cells (CTLs), is to eliminate the antigen infected cells by inducing apoptosis, e.g, through the release of cytotoxins. The primary role of CD4+ T cells, also knowns as helper T cells (Ths), is to secrete the cytokines necessary to further expand the immune response, such as growth signal interleukin-2 (IL-2). Specifically, these secreted cytokines aid in the continual proliferation of CTLs. Moreover, a portion of CD4+ T cells will further differentiate into regulatory T cells (Tregs).

Throughout the immune response, Tregs are responsible for actively suppressing immune cells to prevent autoimmunity, and they continually proliferate in response to the secretion of IL-2 by the antigen-activated T cells. Furthermore, regulatory T cells play a key role in the final stage of an immune response, contraction. Once the CTLs have eliminated the antigen infected cells, through the secretion of inhibitory cytokines, and are no longer needed, Tregs are responsible for eliminating the remaining effector T cells, leading to the full contraction of the adaptive immune response.

1.1.1 Primary vs. Subsequent Immune Responses

There are key differences between a primary immune response and subsequent responses. After a primary response, the immune system is primed to provide an accelerated and amplified secondary and subsequent responses when compared with the primary one. This difference is driven primarily by the presence of antigen specific *memory cells*. These cells, while formed from T cells, require a lower amount of stimulation to be activated. Accordingly, they perform as effector T cells faster than their non-antigen specific naïve counterparts [2]. Moreover, the effector T cells present in a primary response produce the growth factor IL-2, which not only drives the proliferation of mature effector T cells, but also drives the transition of these cells into memory T cells [3, 4]

During a secondary immune response, dormant memory T cells join the effector T cells that come from activated naïve T cells. Since memory cells are more antigen specific, the amount of APC and cytokine stimulation that is required to activate the cells is significantly lower than that of naïve T cells [3, 5, 6]. Memory T cells can be divided into two main compartments: central memory (CM) and effector memory (EM) T cells. When encountered with a secondary infection of an antigen, EM cells require low stimulation for activation, while CM cells require lower stimulation for proliferation [7, 8]. Thus, the two memory cell compartments together allow a faster and stronger effector T cell response. Due to this fast response, it was shown that memory cells are the driving force behind secondary immune responses, with the majority of effector T cells being those derived from dormant memory T cells [9].

Given that dormant memory T cells can have a half-life of up to 8–15 years, these cells allow for a prolonged and effective use of the immune system [10,11]. The formation and efficacy of these memory T cells heavily depends on the duration of antigen exposure and on the strength of the inflammatory signaling. Shortening the duration of antigen exposure by introducing therapies, such as antibiotics, can prevent the formation of memory T cells. In contrast, overexposure to antigen, such as in chronic viral infections, can also prevent the formation of memory T cells through clonal exhaustion—continual antigen stimulation leading to terminally differentiated effector T cells [12].

1.1.2 Memory T Cell Dynamics

There are a two main theories as to when and how antigen specific memory T cells are formed (Kaech and Cui 2012), see Figure 1.1. The first theory assumes that memory T cells differentiate from naïve T cells independently of the effector T cells. Moreover, in this theory, the precursor T cells are primed to be either effector or memory, not both. While possible, it is unlikely that naïve T cells are primed to form either precursor memory cells or effector T cells due to the fact that in Gerlach et al (2010) it has been shown that naïve T cells have the ability to form both T cell subtypes [13].

A second theory of memory T cell differentiation assumes that memory T cells form from effector T cells. As explained in Kaech and Cui (2012), while still differentiating from effector T cells, there are a several mechanisms that could be at

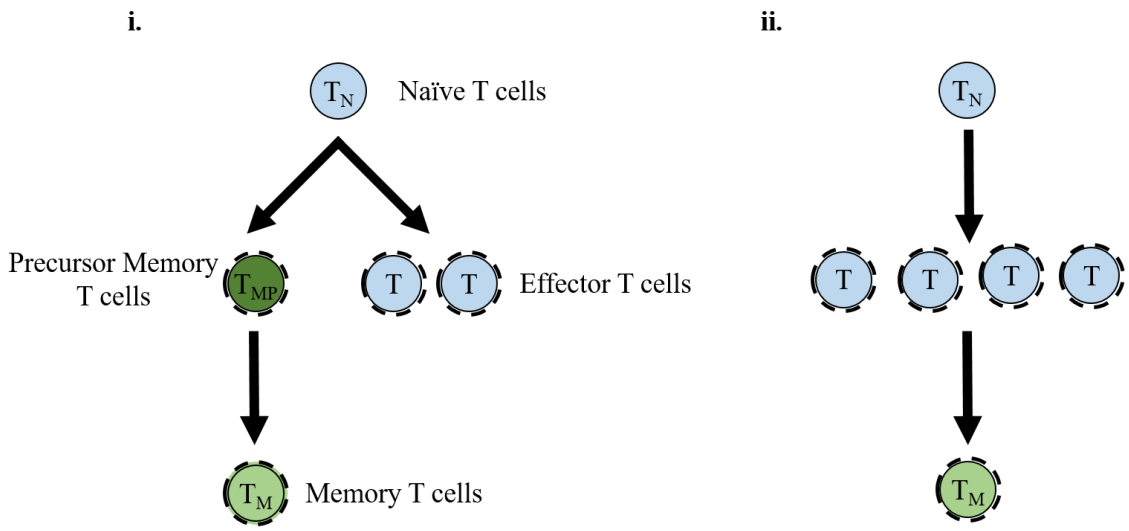

Figure 1.1: Diagram of the formation of memory effector T cells.(i) Memory T cells do not form out of effector T cells. Rather, a percentage of naïve T cells differentiate into precursor memory T cells that further differentiate into memory T cells. (ii) Memory T cells form as a fraction of the effector T cells during the contraction phase of the immune response.

play [12]. First, the decreasing-potential model posits the notion that throughout infection effector T cells keep a history of the signals they receive and will differentiate into the various memory T cells or remain as effector T cells based on these signals. Here, when there is constant signaling and interaction with antigen, cells are more likely to remain effector T cells and terminally differentiate. Similar to the decreasing-potential model, the signal-strength model, or linear differentiation model, suggests that memory T cells differentiate solely based on the strength of the signaling that the effector T cells receive. The main difference between the two effector to memory models is that in the signal-strength model, the fate of the effector T cell can be determined early in the immune response.

There are also less well defined models that do not fall into the main two categories, such as the asymmetric cell fate (ACF) model. The ACF model suggests

that while effector T cells are clonally expanding, based on the type of mature APC-T cell connection, effector T cells can divide asymmetrically into both effector T cells and memory T cells.

In this study, we will assume a memory T cell differentiation model similar to that of the signal-strength model. Here around 5–10% of effector T cells differentiate into dormant memory T cells based on the amount of APC and IL-2 stimulation throughout the entire immune response [12]. With this model of differentiation, just as shown *in vivo*, the majority of memory T cells will differentiate during the contraction phase of the immune response.

1.2 Adaptive Immunity in Chronic Infection

The immunological responses described in Section 1.2 best describe the immune system during acute infections. These infections include encounters with antigen either once or several times within a lifetime with longer periods of time between encountering the same antigen. The immune system's response during an acute infection can vary drastically compared with its response during a chronic infection. During chronic infections, we can view the immune system as encountering the same antigen multiple times. Moreover, chronic infections widely vary in the amount of time between each immune interaction from long spans of time (such as with well-controlled asthma) to short spans (such as in late-stage cancer). In this dissertation we study breast cancer in the dormant phase, which we view as a chronic disease, and a specific immunological consequence of late stage chronic diseases, T cell ex-

haustion.

1.2.1 The Immune System in Breast Cancer Dormancy

One of the primary hallmarks of cancer is metastasis, the ability of tumor cells to break off from the primary tumor, disseminate to a secondary location, and proliferate. These disseminated tumor cells (DTCs) have the ability to evade traditional treatment and immunological response and eventually proliferate at a secondary malignant site. The latency period between remission and relapse, the time in which these metastatic tumors occur, is known as metastatic dormancy [14].

There are two main types of dormancy: cellular dormancy and tumor mass dormancy. Under cellular dormancy, or solitary cell dormancy, a single DTC goes through periods of growth arrest. Due to factors in the host organ microenvironment, these cells enter states of quiescence that, unlike in healthy cells, are usually reversible, allowing for the cells to escape dormancy and restart proliferation. Tumor mass dormancy on the other hand, occurs when the cells of a metastatic tumor are proliferating at the same rate at which they are going through apoptosis, or cell death. This balanced proliferation is caused by two main functions: angiogenesis, the host organ's inability to provide vasculature necessary to supply enough nutrients for the tumor to grow, and immune system induced dormancy. For the purposes of this study, we will focus on immune-induced dormancy.

As stated, immune-induced dormancy takes place when there is a balance between cell growth and the immune system's response. In order for DTCs to

create a lesion at a secondary site, these cells must be able to interact with the cells in the new microenvironment while escaping normal immune system surveillance, or immunoediting. For this reason, the majority of DTCs die due to their inability to survive in the new host environment. However, depending on the cancer type, there are particular niches in which DTCs can coexist with host organ cells in order to remain in long periods of dormancy. In non immune compromised patients, the cancer cells are cleared primarily by the adaptive immune system, specifically cytotoxic T cells, or CD8+ cells. In conjunction with helper T cells, CD4+ cells, and the cytokines produced, these effector T cells have the ability to recognize tumor cells and suppress metastatic lesion spread [15]. Escape from this state of balanced proliferation is thought to be driven by factors internal and external to immunoediting such as environmental stress or immune system deterioration due to aging. With this understanding, prevention of immune-induced dormancy escape may be possible with immunotherapy [16].

When observing breast cancer cells (BCCs), we find that they most readily metastasize to the bone marrow. The bone barrow is a common secondary site for BCCs to disseminate due to a microenvironment that assists the cells in evading the immune system. In the bone marrow, BCCs recruit mesenchymal stem cells which express the cytokine TGF-β1, which suppresses cytotoxic T cells while increasing the number of regulatory T cells [17,18]. Through the recruitment and expansion of Tregs, BCCs are able to partially evade the immune system by active suppression of CTLs via apoptosis and divert innate immune system cells by secreting anti inflammatory cytokines. Consequently, breast cancer cells can remain in the bone

marrow for a long time without being eliminated by the immune system.

1.2.2 T Cell Exhaustion

T cell exhaustion describes the state present during many chronic infections and late stage cancers when T cells lose functionality due to persistent and frequent encounters with antigen cells. The nature of T cell exhaustion occurs in a hierarchical manner [19]. Early in chronic infections, the adaptive immune system acts as it would during an acute infection. As time progresses, with the increase in antigen presentation, T cells slowly lose functionality in the following order. First, T cells begin to lose their ability to secrete IL-2 and CTLs begin to lose their high proliferative capacity. Next, the ability to produce tumor necrosis factor (TNF) depletes, which effects the cancer killing capacity of T cells. The third stage is when CD8+ T cells lose their ability to induce apoptosis. Finally, with high levels of exhaustion, T cells lose all functionality and apoptosis is induced in the effector T cells.

Other than effector T cells, memory T cells are also affected by T cell exhaustion. Although memory T cells may still be able to activate as they normally would during an acute infection, during chronic infections, it is harder for dormant memory T cells to sustain long term due to low expressions of CD122 and CD127 [19]. Moreover, it has been shown that during chronic infections, if memory T cells are present, exhausted memory T cells are maintained via the constant representation of their specific antigen. Thus, without antigen presentation, exhausted memory T cells lose their ability to maintain homeostatic self-renewal. Regardless of whether

exhaustion affects effector or memory T cells, it has been shown that at the cellular level reversing exhaustion is difficult. However, with antigen maintenance via therapy or by blocking exhaustion pathways such as the PD-1 pathway, it has been shown that it is possible to reverse exhaustion as an overall T cell population.

1.3 Outline of Dissertation

The structure of this thesis is as follows. In Chapter 2 we provide an overview of previous mathematical models of adaptive immunity in acute and chronic infections. Specifically, we review models associated with T cell memory development, cancer dormancy, and T cell exhaustion. At the end of the chapter, we focus on the models developed in Kim et al. (2009, 2010, and 2011) and their studies of adaptive immunity activation and regulation [20–22]. These models serve as the primary source for our work.

In Chapters 3, we develop a mathematical model to study T cell driven adaptive immunity in a secondary immune response through the use of memory T cells. We observe the importance of memory T cells in the speed and magnitude of the secondary response and create a framework to build our second and third models. In Chapters 4 and 5 we develop mathematical models to study chronic infections, specifically through the lens of breast cancer dormancy in the bone marrow and the incorporation of T cell exhaustion, respectively.

For our breast cancer dormancy model, we observe the importance of immune protection on the final outcome of the system. We also are able to see the importance

of slow versus fast growing breast cancer cells. For our T cell exhaustion model, our simulations suggest that the most important factors for outcome are, IL-2 production and long term memory maintenance. All models developed are written as systems of delayed differential equations. Finally, in Chapter 6 we discuss further applications and extensions of the models developed in Chapters 3, 4, and 5 and present our final remarks.

Chapter 2: Preliminaries

2.1 Motivation

In recent years, mathematicians have been motivated to create mathematical models that enabled the study and investigation of different immunological processes and phenomena. Beyond theoretical mathematical models, through the help of data, the study of immunology has more readily incorporated *in silico* experiments. Applications of these mathematical models range from studying the mathematical properties of these biological systems to developing new approaches for modulating the immune response, saving resources, and guiding clinical trials. When combining the complementary expertise of immunologists and mathematicians, we expedite advancements in clinical treatments, and improve patient diagnosis and prognosis. Through the flow of expertise and ideas between clinicians, immunologists, and mathematicians, we open the door to better research of complex immunological systems, leading to a better understanding of the multiscale nature of immunology.

2.2 Summary of Mathematical Models

We begin by outlining recent mathematical models that study acute immunology and our primary focuses within chronic immunology—breast cancer dormancy and T cell exhaustion. Though this summary of mathematical models is not exhaustive, we aim to cover a multitude of contributions of the mathematical study of immunology. For a more complete review of relevant mathematical contributions, we refer you to Eftimie et al. (2016) and Wilkie et al. (2013) [23, 24].

2.2.1 Acute Infection

From molecular to tissue-level interactions, there are numerous mathematical models that have been developed to address immunological questions about acute infections [23]. At the molecular level, the majority of mathematical models are created to study innate immunity in comparison to models for adaptive immunity. However, in recent years there has been progress in the study of two specific areas of molecular-level dynamics: (1) T cell receptor (TCR) and B cell receptor (BCR) binding; (2) signaling pathways used for cellular functionality.

TCR and BCR binding is either modeled by deterministic ordinary differential equations (ODEs) or by stochastic models. They explore the mechanisms driving TCRs binding to major histocompatibility complex (MHC) molecules and BCRs binding to antigens [25]. Specifically, these models aim to gain insight into the molecular activation of T cells and B cells as well as understanding the overall diversity in the amount and size of these receptors from cell to cell. Signaling pathways

research aims to study and quantify the signally pathways between immune cells. Whether the models are relatively short, describing individual phenomenon like the NF-κB pathway or pathways in metabolism in immune cells [26] , or more complex, such as with the exploration of the signaling pathway for BCR-antigen binding in Barua et al. (2012) [27], the majority of these models are written as ODEs.

At the cellular level, for innate immunity there are investigations into bacterial infections, viral infections, and the combination of viral and bacterial infections. The mathematical tools used vary widely. They include ODEs, partial differential equations (PDEs), and stochastic models. In contrast, models addressing T cell differentiation [13, 28], T cell movement [29], and T cells in viral [30] and bacterial infections [31] all explore various dynamics of adaptive immunity.

In primary immune response, models developed by Kim, Lee, and Levy (2009, 2010, 2011) and Wilson and Levy (2013) explore T cell expansion and regulation as well as the effects of regulatory T cell switching on immune contraction. Recent studies have also looked into the generation of memory cells and their differentiation [30, 32]. Juxtaposed to the mathematical models created to study innate immunity, most of the models studying adaptive immunity are simple ODE models. Also, these models focus mainly on primary immune response and the generation of cells following primary antigen stimulation.

Considering that there are immunological processes occurring at the tissue level, where individual cells combine to form multicellular structures, mathematical models have also been developed to understand such phenomena. In contrast to the models developed at the molecular and cellular level, the majority of these

models contain a spatial element and are modeled as PDEs, agent-based models, and cellular automata. Examples of mathematical contributions at the tissue-level include wound healing, tumor-immune dynamics, formation of granulomas, and the formation of micro-abscesses post bacterial infection.

Given that the majority of interactions at the tissue level incorporate interactions at the cellular and molecular level, the majority of the resulting mathematical models can also be considered multiscale models. Multiscale models extend from finding the relationship between molecular-level and cellular-level agents to studying how the relationship between cells affects infection spread at the population level. We note that the majority of these models aim to study the ways in which molecular processes affect cellular dynamics, such as how the NF-κB pathway as well as TNF cytokine secretion affect the inflammatory response of burn injuries [33]. Given that our research focuses on understanding the dynamics of memory T cell formation, activation, and regulation, we will take a cellular approach to modeling acute immunology.

2.2.2 Cancer Dormancy

While there are many mathematical models for tumor-immunology and immunotherapy, there are very few mathematical models that specifically addressed immune-induced cancer dormancy. The majority of these models are simple ODE models with few cellular compartments, generally incorporating cancer cell populations, quiescent and proliferating, and an all encompassing immune cell popula-

tion [34–36]. Due to the simplified nature of these models, the authors are able to complete thorough parameter analyses to draw information about the causes of cancer.

A more complex example of modeling dormancy is found in Kuznetsov (1988), where the author uses a system of a mixture of delayed differential equations (DDEs) and ODEs to model the interaction between immune cells and tumor cells [37]. While not cancer specific, the model incorporates cells from both innate and adaptive immunity and is written as follows:

$$\frac{dT}{dt} = T(c_1 - c_2C - c_3N), \tag{2.1}$$

$$\frac{dN}{dt} = j_N - c_4N - c_5NT, \tag{2.2}$$

$$\frac{dS}{dt} = \frac{c_6T}{1 + \frac{T}{c_7}} - c_8S, \tag{2.3}$$

$$\frac{dP}{dt} = \frac{c_9CT}{c_{10} + S}c_{11}P - c_{12}PT, \tag{2.4}$$

$$\frac{dC}{dt} = c_{13}H(t-\tau)P(t-\tau) + \frac{jc}{1 + \frac{S}{c_{14}}} - c_{15}CT - c_{16}C. \tag{2.5}$$

Here the cell compartments are divided into tumor cells (T), natural killer cells (N), suppressor cells (S), memory cells (P), and cytotoxic T cells (C). H is a Heaviside function whose role is to turn on the production of cytotoxic T cells after time τ. They conclude that without cytotoxic T cell (CTL), no dormant state exists, while a dormant state can exist after CTL activation. Moreover, he introduces what is known as the an *immune barrier*, which are conditions that guide tumor growth based on the rate of growth of tumor cells, the concentration of tumor cells, and

the concentration of immune cells. From a biological perspective, it is now known that some of the assumptions made in the model are incorrect. For example, though memory cells have the same capabilities as ordinary effector T cells, they have the ability to respond to antigen more rapidly and amplify the amount of immune cells present more than effector T cells.

2.2.3 T Cell Exhaustion

Similarly to cancer dormancy models, there have been few contributions specifically addressing T cell exhaustion. An early study into the dynamics of T cell exhaustion by Wodarz et al. (1998) involved studying the interaction between cytotoxic T cells (CTLs) and virus-infected cells [38]. They observe T cell exhaustion as a product of the dynamics of the system and its parameter values as opposed to incorporating the exhaustion directly into the model. A more recent model by Johnson et al (2011) of T cell responses studies T cell exhaustion through its own model compartment [39]. This model follows the interactions between uninfected target cells (U), virus-infected target cells (V), the magnitude of the immune response (X), and the amount of exhaustion in the system (Q). The model is written as follows:

$$\frac{dU}{dt} = a - \beta UV - bU, \tag{2.6}$$

$$\frac{dV}{dt} = \beta UV - (b + \alpha)V - kVX, \tag{2.7}$$

$$\frac{dX}{dt} = sX\frac{V}{\theta + V} - \delta X\frac{Q^n}{q_c^n + Q^n}, \tag{2.8}$$

$$\frac{dQ}{dt} = \frac{V}{\theta + V} - d_q Q. \tag{2.9}$$

Given that the effect of exhaustion on the immune response is driven by the Hill equation, $\frac{Q^n}{q_c^n + Q^n}$, the dynamics of the system heavily depend on the value of the exhaustion threshold parameter, q_c. We observe infection clearance with high values of q_c, while with low values of this parameter, we see the immune response being eliminated and the infected cells take over the system. As a result, the authors are able to use this model to further investigate the ways in which vaccinations change these outcomes by adding in more CTLs. While certainly insightful about the effects of T cell exhaustion, they do not incorporate a pertinent characteristic of T cell exhaustion: the effects of exhaustion happen in a hierarchical way, reducing different T cell functions of different T cell subtypes with increased amounts of exhaustion.

2.3 Modeling Immune Regulation

We now focus on a series of mathematical models developed by Kim, Lee, and Levy (2009, 2010) and Wilson and Levy (2013) [21, 22, 40]. Their models are written as a system of delayed differential equations (DDEs). The primary focus of these models were to provide insight into T cell driven adaptive immunity and the generation, regulation, and contraction of these cells during a primary immune response. For each of these models, we provide a detailed description and main conclusions. These models are used as a basis for the formation of our three adaptive

immunity models (See Chapters 3, 4, and 5).

2.3.1 Modeling the Immune Response after a Primary Infection (Kim, Lee, and Levy 2009)

Kim et al. (2009) develop three models in order to better understand the expansion and contraction of T cells. While the initial activation of naïve T cells is consistent between all three models, the difference between the models lie in the ways in which the T cell response contracts. The first two models assume that there is a built-in mechanism of apoptosis within each cell which leads to the contraction of the T cell immune response to antigen. They model this behavior in two ways. A cell division-based program is assumed for the first model, where after a maximum number of divisions, the T cell awaits for apoptosis.

In contrast, in the second model they assume a time-based program, where T cells contract after a set amount of time. Both models are shown to have a major deficiency, namely the linear response to the precursor frequency upon the initial viral exposure. This leads to the third model, that does not assume that immune response contraction is a proportional internal mechanism of the individual T cell; rather, they assume that there is a negative feedback loop created by regulatory T cells (Tregs). We outline the third model below:

$$\dot{A}_0 = s_A - d_0 A_0(t) - a(t) A_0(t), \tag{2.10}$$

$$\dot{A}_1 = a(t) A_0(t) - d_1 A_1(t), \tag{2.11}$$

$$\dot{T_0} = s_T - \delta_0 T_0(t) - kA_1(t)T_0(t), \tag{2.12}$$

$$\dot{T_1} = 2^m kA_1(t-\sigma)T_0(t-\sigma) - kA_1(t)T_1(t) + 2kA_1(t-\rho)T_1(t-\rho)$$
$$- (\delta_1 + r)T_1(t) - kT_R(t)T_1(t), \tag{2.13}$$

$$\dot{T_R} = rT_1(t) - \delta_1 T_R. \tag{2.14}$$

Here, A_0 and A_1 represent the concentration of immature and mature antigen presenting cells (APCs) at the site of infection, respectively. A_1 are assumed to begin displaying antigen and travel to the lymph nodes to activate the naïve T cells present, T_0. T_1 represent the concentration of effector T cells, or mature T cells. And finally, T_R represents the concentration of Tregs derived from effector T cells.

With all three models, Kim et al. explore the paradigm of having a minimal T cell developmental program following initial APC activation. Specifically, they assume that following activation, each cell must undergo antigen-independent proliferation for a set number of times before they are fully mature effector T cells. Once mature, they continue with antigen-dependent proliferation until apoptosis. In the DDE models, the developmental program is achieved by allowing cells to undergo the division, producing 2^m copies in σ time. The third model provides a nonlinear response to changes in the initial amount of precursors, due to the incorporation of Tregs. Several follow-up papers improved the regulation of the system and the robustness with respect to the precursor frequency.

2.3.2 Modeling Immunodominance (Kim, Lee, and Levy 2010)

Immundominance is a phenomenon that occurs when T cells respond to antigen epitopes in a hierarchical manner. Given that antigens can contain multiple epitopes, T cells respond to dominant epitopes first, and following the contraction of the epitope specific T cell, the less dominant epitope specific T cells emerge. The model developed by Kim et al. (2010) aims to explore the two differing theories of immunodominance, regarding the competition between T cells. The first theory assumes that T cells take part in passive competition due to limited resources. The second theory assumes active competition, where the competition is driven by the active suppression of other T cells.

Kim et al. argue in favor of active competition and expand their immune regulation model (Kim et al. 2009). They expand the T cell compartment to include both helper T cells (Ths) and cytotoxic T cells (CTLs). Furthermore, in order to better mediate the growth and regulation of T cells, they incorporate the growth signal cytokine, interleukin-2 (IL-2). This leads to the following model:

$$\dot{A}_0 = s_A - d_0 A_0(t) - a(t)A_0(t), \tag{2.15}$$

$$\dot{A}_1 = a(t)A_0(t) - d_1 A_1(t), \tag{2.16}$$

$$\dot{H}_i^0 = s_{H,i} - \delta_0 H_i^0(t) - k_i A_1(t) H_i^0(t), \tag{2.17}$$

$$\begin{aligned}\dot{H}_i = {} & 2^{m_1} k_i A_1(t-\sigma_1) H_i^0(t-\sigma_1) - k_i A_1(t) H_i(t) + 2k_i A_1(t-\rho_1) H_i(t-\rho_1) \\ & - (\delta_H + r) H_i(t) - k R_{total}(t) H_i(t),\end{aligned} \tag{2.18}$$

$$\dot{K}_i^0 = s_{K,i} - \delta_0 K_i^0(t) - k_i A_1(t) K_i^0(t), \tag{2.19}$$

$$\dot{K}_i = 2^{m_2} k_i A_1(t-\sigma_1) K_i^0(t-\sigma_1) - kP(t)K_i(t) + 2kP(t-\rho_2)K_i(t-\rho_2)$$
$$- \delta_k K_i(t) - kR_{total}(t)K_i(t), \tag{2.20}$$

$$\dot{P} = r_1 H_{total}(t) + r_2 K_{total}(t) - \delta_P P(t) - kP(t)K_{total}(t) - kP(t)R_{total}(t), \tag{2.21}$$

$$\dot{R}_i = rH_i(t) - kP(t)R_i(t) + 2kP(t-\rho_1)R_i(t-\rho_1) - \delta_H R_i(t), \tag{2.22}$$

where $\sum H_i = H_{total}$, $\sum K_i = K_{total}$, and $\sum R_i = R_{total}$ for $i = 1, ..., n$. Here, A_0 and A_1 represent the concentration of immature APCs at the site of infection and mature APCs that are presenting antigen in the lymph nodes, respectively. For each clone i, H_i^0 represents the concentration of naïve helper T cells and H_i is the concentration of mature helper T cells. Similarly, K_i^0 and K_i represent the concentration of naïve and mature cytotoxic T cells, respectively. Finally, R_i represents regulatory T cell concentration and P represents IL-2 concentration. Immunodominance is shown to emerge due to the non-specific response of the iTregs.

2.3.3 Reverse Transitions of Regulatory Cells to Helper Cells (Wilson and Levy 2013)

The primary focus of this work was to study the way in which regulatory T cells are developed. The authors take two modeling approaches. The model is based on Sakaguchi (2008, 2010) in which it was suggested the regulatory cells may reverse their functionality and function as helper T cells [41, 42]. This transition is

incorporated into the Kim et al. (2010) model. The extended model is the following:

$$\dot{A}_0 = s_A - d_0 A_0(t) - a(t)A_0(t), \tag{2.23}$$

$$\dot{A}_1 = a(t)A_0(t) - d_1 A_1(t), \tag{2.24}$$

$$\dot{H}^0 = s_H - \delta_0 H^0(t) - kA_1(t)H^0(t), \tag{2.25}$$

$$\begin{aligned}\dot{H} &= 2^{m_1} kA_1(t-\sigma_1)H^0(t-\sigma_1) - kA_1(t)H(t) + 2kA_1(t-\rho_1)H(t-\rho_1) \\ &\quad + \mu\frac{R(t)}{1+dP(t)} - (\delta_H + r)H(t) - kR(t)H(t),\end{aligned} \tag{2.26}$$

$$\dot{K}^0 = s_k - \delta_0 K^0(t) - kA_1(t)K^0(t), \tag{2.27}$$

$$\begin{aligned}\dot{K} &= 2^{m_2} kA_1(t-\sigma_1)K^0(t-\sigma_1) - kP(t)K(t) + 2kP(t-\rho_2)K(t-\rho_2) \\ &\quad - \delta_k K(t) - k_E R(t)K(t),\end{aligned} \tag{2.28}$$

$$\dot{P} = r_1 H(t) + r_2 K(t) - \delta_P P(t) - kP(t)K(t) - kP(t)R(t), \tag{2.29}$$

$$\dot{R} = rH(t) + 2kP(t-\rho_1)R(t-\rho_1) - kP(t)R(t) - \mu\frac{R(t)}{1+dP(t)} - \delta_H R(t). \tag{2.30}$$

Here, A_0 represents the concentration of immature APCs at the site of infection, while A_1 is the concentration of mature APCs that are presenting antigen in the lymph nodes. H^0 and H represent the concentrations of naïve and mature helper T cells, respectively. Similarly, K^0 and K represent the concentration of naïve and mature cytotoxic T cells, respectively. Finally, P represents interleukin-2 concentration and R represents regulatory T cell concentration.

Incorporating the reverse transition of Tregs back to helper T cells is shown to better scale the response of the mature T cells with the initial precursor populations, essentially resulting with a more robust model than the previous models.

They conclude that those two captured features of Treg switching may be major contributers to overall adaptive immunity dynamics.

Chapter 3: Adaptive Memory in Primary and Secondary Immune Response

3.1 Overview

During an acute immune response, it is understood that there are key differences between the cells and cytokines that are present in a primary response and those present in subsequent responses. Specifically, memory cells that remain after a primary response drive the clearance of antigen in later encounters. We begin by assessing previous mathematical models discussed in Section 2.3. In Kim et al. (2010), the authors develop a mathematical model that allows for generation, regulation, and activation of T cells. However, given that the focus of this study was on primary response, when extended to incorporate a secondary encounter with the same antigen, the Kim model performs essentially the exact way as it does with the primary response (see Figure 3.1). This result is not biologically accurate given that in acute secondary and subsequent immune responses, the presence of memory T cells accelerates the response.

In this chapter, we develop a mathematical model to explore the differences between the primary and secondary immune responses through the creation, acti-

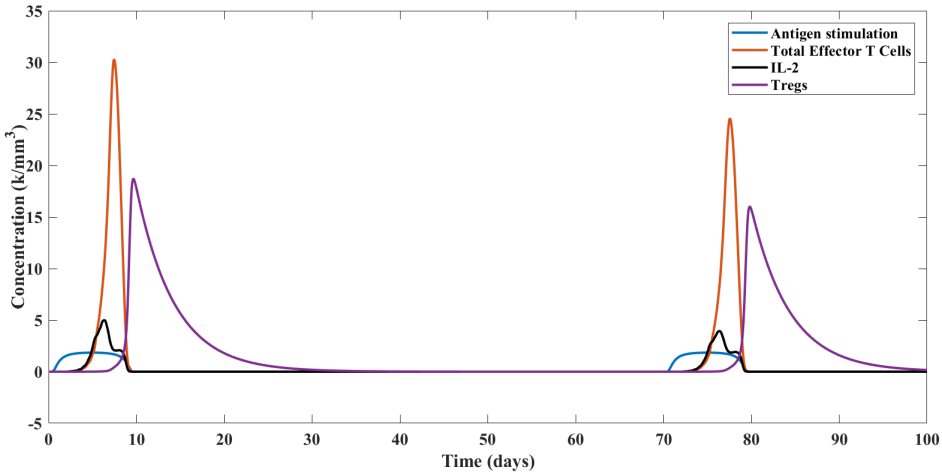

Figure 3.1: The dynamics the Kim et al.(2010) model with a primary and secondary immune response. In the absence of memory cells, we observe similar levels of the immune cells when responding to the same antigen.

vation, and regulation of memory T cells. We mimic this biological behavior with a delay differential equation (DDE) model of both primary and secondary immune responses to the same antigen. While we observe similar amounts of antigen stimulation from both immune responses, with the incorporation of memory T cells, we see an increase in the amount of effector T cells present as well as in the speed of activation of the immune system in the secondary response. We conclude that with this mathematical model, we can capture the desired secondary immune response dynamics.

3.2 Adaptive Memory Model

Following the framework developed in Kim et al. (2010), we develop a delayed differential equation model which incorporates memory T cells and an antigen compartment that is responsive to the immune cells present in the system. As defined in Section 1.1.2, we combine central memory (CM) and effector memory (EM) cells

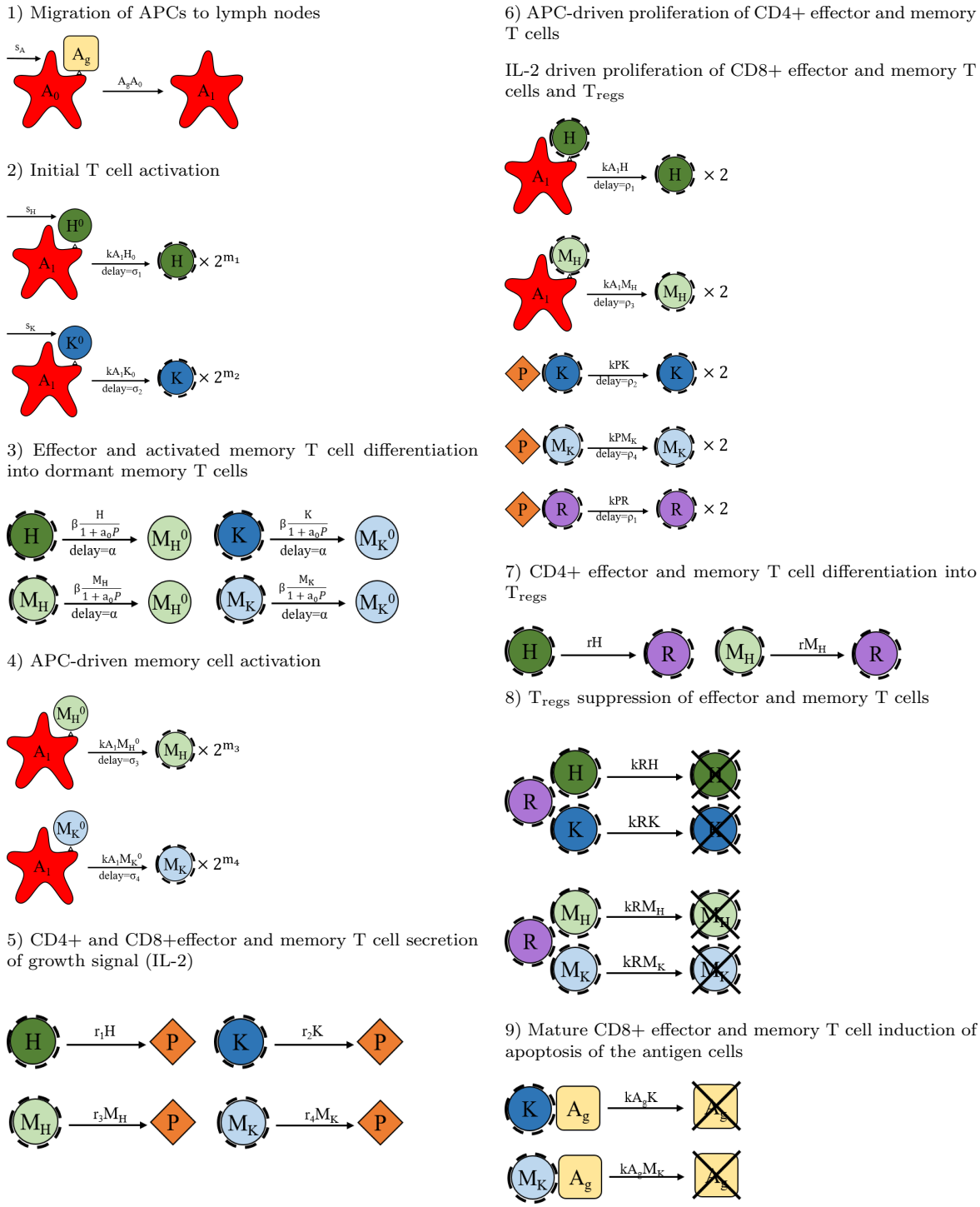

Figure 3.2: Diagram of adaptive immunity model with memory cells (3.1)-(3.13). The compartments are represented as follows: A_0: immature APCs, A_1: mature APCs, H^0: naïve helper T cells, H: mature helper T cells, K^0: naïve cytotoxic T cells, K: mature cytotoxic cells, M_H^0: dormant memory helper T cells, M_H: activated memory helper T cells, M_K^0: dormant memory cytotoxic T cells, M_K: activated memory cytotoxic cells, P: IL-2 concentration, R: regulatory T cells, and A_g: antigen concentration.

into a singular memory T cell compartment that both responds to antigen with less stimulation and clonally expands faster than their non-memory counterparts. We also extend the scope from primary immune response to both primary and secondary immune responses. Our model is shown in Figure 3.2, and includes the following elements:

1. Immature APCs, $A_0(t)$, become mature APCs, $A_1(t)$ when they interact with antigen, $A_g(t)$. Mature APCs travel to the lymph nodes.

2. In the lymph nodes, the naïve helper T cells, $H^0(t)$, and naïve cytotoxic T cells, $K^0(t)$, interact with the mature APCs and begin to undergo the minimal developmental program. Here the helper T cells and the CTLs divide m_1 and m_2 times, respectively, for the duration of σ_1 and σ_2, respectively.

3. In primary immune response, during the contraction phase, when the amount of mature APCs, $A_1(t)$, is low, mature helper T-cells and mature CTLs, transition into dormant memory helper cells, $M_H^0(t)$, and dormant memory CTLs, $M_K^0(t)$, respectively. In the contraction phase of secondary and subsequent immune responses, mature helper T cells and activated memory helper cells, $M_H(t)$, both transition to $M_H^0(t)$. Similarly, mature CTLs and activated memory CTLs, $M_K(t)$, both transition to $M_K^0(t)$ during the contraction phase of secondary and subsequent immune responses. The duration of the transition into $M_H^0(t)$ and $M_K^0(t)$ is α.

4. In secondary and subsequent immune responses, the dormant memory T cells, interact with mature APCs causing them begin the minimal developmental

program. Here the memory helper T cells and the memory CTLs divide m_3 and m_4 times, respectively, for the duration of σ_3 and σ_4, respectively.

5. Both mature effector T cells and activated memory T cells secrete the growth signal IL-2, $P(t)$.

6. Once mature T cells and activated memory T cells complete the minimal developmental program, they become effector T cells and continue to divide. The CD4+ cells continue to proliferate in response to an interaction with the mature APCs, while CD8+ cells proliferate in response to stimulation by IL-2.

7. A proportion of mature helper T cells and activated memory helper cells transition into regulatory T cells in response to stimulation by antigen.

8. Regulatory T cells suppress mature effector T cells as well as activated memory T cells. They also proliferate in response to IL-2 stimulation.

9. Mature CTLs and activated memory CTLs induce apoptosis in antigen cells.

The model for adaptive immunity dynamics including memory cells is given by the following equations:

$$\dot{A}_0 = s_A - d_0 A_0(t) - A_g(t) A_0(t), \tag{3.1}$$

$$\dot{A}_1 = A_g(t) A_0(t) - d_1 A_1(t), \tag{3.2}$$

$$\dot{H}^0 = s_H - \delta_0 H^0(t) - k A_1(t) H^0(t), \tag{3.3}$$

$$\dot{H} = 2^{m_1} k A_1(t-\sigma_1) H^0(t-\sigma_1) - k A_1(t) H(t) + 2kA(t-\rho_1) H(t-\rho_1)$$

$$- (\delta_H + r)H(t) - kR(t)H(t) - \beta\frac{H(t)}{1 + a_0P(t)}, \tag{3.4}$$

$$\dot{K}^0 = s_k - \delta_0K^0(t) - kA_1(t)K^0(t), \tag{3.5}$$

$$\dot{K} = 2^{m_2}kA_1(t-\sigma_2)K^0(t-\sigma_2) - kP(t)K(t) + 2kP(t-\rho_2)K(t-\rho_2) - \delta_kK(t)$$

$$- k_ER(t)K(t) - \beta\frac{K(t)}{1 + a_0P(t)}, \tag{3.6}$$

$$\dot{M}_H^0 = \beta\frac{H(t-\alpha)}{1 + a_0P(t-\alpha)} + \beta\frac{M_H(t-\alpha)}{1 + a_0P(t-\alpha)} + (r_{MH} - \delta_{MH})M_H^0(t)$$

$$- k_{MH}A_1(t)M_H^0(t), \tag{3.7}$$

$$\dot{M}_H = 2^{m_3}k_{MH}A_1(t-\sigma_3)M_H^0(t-\sigma_3) - kA_1(t)M_H(t) + 2kA_1(t-\rho_1)M_H(t-\rho_1)$$

$$- (\delta_H + r)M_H(t) - kR(t)M_H(t) - \beta\frac{M_H(t)}{1 + a_0P(t)}, \tag{3.8}$$

$$\dot{M}_K^0 = \beta\frac{K(t-\alpha)}{1 + a_0A_1(t-\alpha)} + \beta\frac{M_K(t-\alpha)}{1 + a_0P(t-\alpha)} + (r_{MK} - \delta_{MK})M_K^0(t)$$

$$- k_{MK}A_1(t)M_K^0(t), \tag{3.9}$$

$$\dot{M}_K = 2^{m_4}k_{MK}A_1(t-\sigma_4)M_K^0(t-\sigma_4) - kP(t)M_K(t) + 2kP(t-\rho_2)M_K(t-\rho_2)$$

$$- \delta_kM_K(t) - k_ER(t)M_K(t) - \beta\frac{M_K(t)}{1 + a_0P(t)}, \tag{3.10}$$

$$\dot{P} = r_1H(t) + r_2K(t) + r_3M_H(t) + r_4M_K(t) - \delta_PP(t)$$

$$- kP(t)K(t) - kP(t)M_K(t) - kP(t)R(t), \tag{3.11}$$

$$\dot{R} = r(H(t) + M_H(t)) + 2kP(t-\rho_1)R(t-\rho_1) - kP(t)R(t) - \delta_HR(t), \tag{3.12}$$

$$\dot{A}_g = [(r_A - \delta_A)A_g(t) - k_AA_g(t)K(t) - k_AA_g(t)M_K(t)] \times \theta(A_g(t) - 10^{-18}) + a(t). \tag{3.13}$$

A_0 represents the concentration of immature APCs at the site of infection, while A_1 is the concentration of mature APCs that are presenting antigen in the

lymph nodes. H^0 represents the concentration of naïve helper T cells and H is the concentration of mature helper T cells. Similarly, K^0 and K represent the concentration of naïve and mature cytotoxic T cells, respectively. M_H^0 and M_H represent the concentration of dormant and activated memory helper T cells, while M_K^0 and M_K represent the concentration of dormant and activated memory cytotoxic T cells. Finally, P represents IL-2 concentration, R represents regulatory T cell concentration, and A_g represents antigen concentration.

Equation (3.1) describes the immature APCs that are available in the body to respond to antigen stimulation. We assume is a constant supply rate of the cells, s_A, and a death rate, d_0, that is proportionate to the amount of immature APCs. Immature APCs are stimulated by the antigen in the system, A_g, and through this stimulation immature APCs become the mature APCs in the lymph nodes described by (3.2). Mature APCs also have a death rate proportional to the amount of mature APCs in the system, d_1.

Equations (3.3) and (3.5) describe naïve T cell populations for helper T cells and cytotoxic T cells, respectively. Both populations have constant supply rates, s_H and s_K, and a death rate, δ_0, that is proportional to the amount of each of the naïve T cell populations. These naïve T cells transition into their respective effector T cell populations based on the mass action interaction with mature APCs.

The mature helper T cell population is described by Equation (3.4). After the naïve CD4+ cells become activated by mature APCs, the first term shows the rate at which they enter the minimal development program where they undergo m_1 cell divisions. The amount of time required for this development program is

characterized by the time delay σ_1. Once the cells are fully mature, CD4+ cells are further stimulated by APCs and proliferate, the rate at which this division occurs is shown by the second and third terms. The amount of time required for a mature helper T cells to divide is represented by the time delay ρ_1. Mature helper T cells are removed from the system by either natural cell death, δ_H, differentiation into regulatory T cells, r, regulatory T cells suppression, or differentiation into dormant memory cells. Since we assume that dormant memory cells are formed during the contraction phase of an immune response, the last term shows the rate of CD4+ cells switching to dormant memory cells occurring when the amount of IL-2 is low.

Equation (3.6) describes the mature cytotoxic T cell population. Similar to the mature helper T cells, the first term shows the rate at which naïve CD8+ cells enter the mature cell population after undergoing the minimal developmental program of m_2 cell divisions. The amount of time required for this developmental is given by the time delay of ρ_2. Further proliferation of CD8+ cells is activated by IL-2, the second and third terms, with the duration of one cell division of CD8+ cells shown by the time delay ρ_2. CD8+ cells exit the system by either natural cell death, δ_K, suppression by regulatory T cells, or by differentiating into dormant memory CTLs when the amount of IL-2 is low, or during the contraction phase.

Equations (3.7) and (3.9) describe the dormant helper and CTL memory cells, respectively. The first two terms of each equation show the rates at which cells are transitioning from either their respective mature T cell populations or their respective activated memory T cell compartment. We assume that after transition from the effector T cell compartments, dormant memory T cells can be activated

only after a time (α) passes. The third terms describe the proportionate growth rate, r_{M*}, and natural death rate, δ_{M*}. The final terms describe the rates at which dormant cells become activated. Similar to naïve T cells, dormant memory cells become activated based on the mass action interaction with mature APCs.

The activated memory T cell populations are described by Equations (3.8) and (3.10), representing CD4+ and CD8+ T cells, respectively. Similar to the activation of non-memory T cells, after the dormant memory cells become activated by mature APCs, the first term shows the rate at which they enter the minimal developmental program where they undergo m_3 and m_4 cell divisions. The amount of time required for this developmental program is characterized by the time delay σ_3 and σ_4. Once the cells are fully activated, CD4+ cells are further stimulated by APCs and proliferate, while CD8+ cells are further stimulated by IL-2. The amount of time required for activated memory CD4+ and CD8+ T cells to divide is represented by the time delay ρ_1 and ρ_2, respectively.

Activated memory CD4+ T cells are removed from the system by either natural cell death, δ_H, differentiation into regulatory T cells, r, regulatory T cells suppression, or differentiation into dormant memory cells. Similarly, activated memory CD8+ T cells are removed from the system by either natural cell death, δ_K, regulatory T cells suppression, or differentiation into dormant memory cells. Since we assume that dormant memory cells are formed during the contraction phase of an immune response, the last term of both equations shows the rate of activated memory cells switching to dormant memory cells occurring when the amount of IL-2 is low.

Equation (3.11) describes the amount of IL-2 in the system. The first four terms show the rate at which IL-2 is secreted by mature helper t cells (r_1), mature CTLs (r_2), activated memory helper T cells (r_3), and activated memory CTLs (r_4). The cytokine has a decay rate, δ_P, proportionate to its amount. IL-2 is also consumed by mature CTLs, activated memory CTLs, and Tregs, given by the last three terms.

The dynamics of regulatory T cells is governed by equation (3.12). The first term gives the rate at which mature helper T cells and activated memory T cells differentiate into Tregs. The next two terms describe the rate at which Tregs further proliferate based on IL-2 activation, with the duration of one Treg cells division characterized by the time delay ρ_1. Tregs exit the system by the same natural death rate of helper T cells, δ_H.

The final equation, (3.13), describes the dynamics of antigens. The first term describes their proportionate growth rate, r_A, and death rate, δ_A. Antigens are removed from the system via interaction with mature CTLs and activated memory CTLs, the second and third term, respectively. $\theta(t)$ is the Heaviside equation, with

$$\theta(t) = \begin{cases} 0 & t < 0, \\ \frac{1}{2} & t = 0, \\ 1 & t > 0. \end{cases}$$

Here, the Heaviside equation prevents the antigen compartment from changing once its population falls below a threshold which we set as 10^{-18} K/mm^3. Consequently,

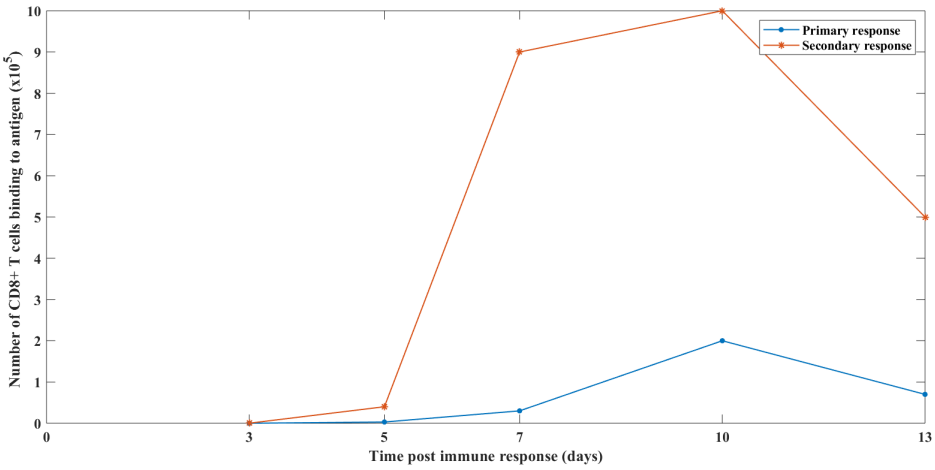

Figure 3.3: Using data from Flynn et el. (1998) [43], we observe the number of active CD8+ T cells present in primary response and secondary response to influenza A virus measured at 3, 5, 7, 10, and 13 days post infection.

this addition reduces the amount of consistent stimulation of the immune cells in the model. Finally, the last term, $a(t)$, describes the source of antigens, which is used to induce secondary immune response during simulation of the model.

3.3 Numerical Results

Using the data of Flynn et al. (1998) [43], we fit our model parameters to mimic the behavior of CD8+ T cells in a primary versus secondary immune response to influenza A (see Figure 3.3). Using the parameter values shown in Table 3.1 we solve Eqs. (3.1)-(3.13) numerically. All simulations were carried out using the MATLAB solver DDESD and the cell concentrations are measured in thousands of cells per cubic mm of blood (K/mm^3). The majority of the parameters used the values found in Kim et al. (2010) and Wilson et al. (2013). Assumptions that are made for these simulations are as follows:

Parameter	Description	Estimate	Source
$A_0(0)$	Initial concentration of immature APCs	10	Kim
$H_0(0)$	Initial concentration of naïve CD4+ T cells	0.06	Kim
$K_0(0)$	Initial concentration of naïve CD8+ T cells	0.04	Kim
s_A	Supply rate of immature APCs	0.3	Kim
d_0	Death rate of immature APCs	0.03	Kim
d_1	Death rate of mature APCs	0.8	Kim
s_H	Supply rate of naïve CD4+ T cells, respectively.	0.0018	Wilson
s_K	Supply rate of naïve CD8+ T cells, respectively.	0.0012	Wilson
k	Kinetic coefficient	5	Wilson
δ_0	Death rate of naïve T cells	0.03	Wilson
δ_H, δ_K	Death rate of mature CD4+ and CD8+ T cells, respectively.	0.23, 0.4	Wilson
m_1, m_2	Number of divisions in the minimal developmental program for naïve CD4+ and CD8+ T cells, respectively.	2, 7	Wilson
σ_1, σ_2	Duration of the minimal developmental program for naïve CD4+ and CD8+ T cells, respectively.	1.46, 4	Wilson
ρ_H, ρ_K	Duration of one T cell division for mature CD4+ and CD8+ T cells, respectively	11/24, 1/3	Wilson
k_E	Kinetic coefficient for CTL-Treg interactions	20	Wilson
β	Rate of differentiation of mature effector T cells into dormant memory effector T cells	0.3	estimated
α	Duration of time for cells to switch into dormant memory effector T cells	25	estimated
r_{MH}, r_{MK}	Growth rate of dormant memory CD4+ and CD8+ T cells, respectively.	0, 0	assumed
δ_{MH}, δ_{MK}	Death rate of dormant memory CD4+ and CD8+ T cells, respectively.	0, 0	assumed
k_{MH}, k_{MK}	Kinetic coefficient for mature APC-memory T cell interactions	5, 5	estimated
m_3, m_4	Number of divisions in the minimal developmental program for dormant memory CD4+ and CD8+ T cells, respectively.	3, 8	estimated
σ_3, σ_4	Duration of the minimal developmental program for dormant memory CD4+ and CD8+ T cells, respectively.	1, 3	estimated
a_0	Magnitude of dependence of dormant memory T cell differentiation on IL-2	5	estimated
r_1, r_2	Rate of IL-2 secretion by mature CD4+ and CD8+ T cells, respectively	10, 1	Kim
r_3, r_4	Rate of IL-2 secretion by activated memory CD4+ and CD8+ T cells, respectively	12.3, 3.3	estimated
δ_P	Decay rate of free IL-2	5.5	Wilson
r	Rate of differentiation of mature and activated memory CD4+ T cells into regulatory T cells	10	estimated
r_A	Growth rate of antigen cells	1	estimated
δ_A	Death rate of antigen cells	0.4	estimated
k_A	Kinetic coefficient for CTL-antigen interactions	2	estimated

Table 3.1: Estimates of parameters for model (3.1)-(3.13). All concentrations are measured in K/mm^3 and time is in days. Initial conditions not provided in the table are zero.

1. We choose to remove the transition of Tregs back to the helper T cell compartment found in Wilson et al. (2013)

2. Memory T cells are slow growing and slow dying; specifically, they proliferate and go through natural cell death at the same rate.

3. Activated memory T cells produce IL-2 ten times more than their non-memory counterparts.

4. Memory T cells have the same kinetic coefficients with IL-2 and mature APCs as their non-memory counterparts, i.e. k, k_{MH}, and k_{MK} are all the same value.

5. The secondary antigen stimulation is the same as the primary stimulation. Moreover, in order to induce both primary immune response and a secondary immune response 300 days later, we set the function $a(t)$ in our antigen compartment to the following:

$$a(t) = \begin{cases} 2 & 0 \leq t < 1, \\ 2 & 300 \leq t < 301, \\ 0 & otherwise. \end{cases}$$

The number 300 is arbitrary. Similar responses occur for any number greater than 25, corresponding to the delay in the reactivation of memory cells.

Figure 3.4 shows the antigen compartments for both primary and secondary responses. We see an indication that the antigen is cleared faster in the secondary

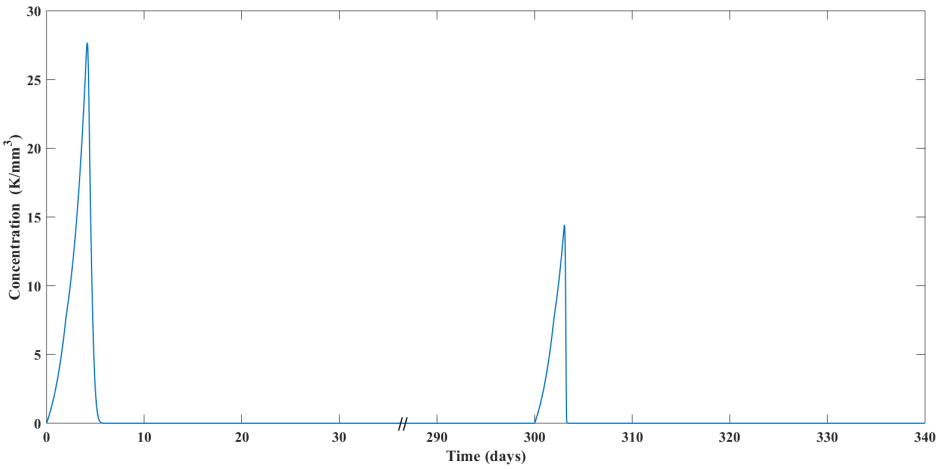

Figure 3.4: The dynamics of antigen cells. We observe a decrease by half in the amount of time required for antigen clearance from the primary to the secondary immune response.

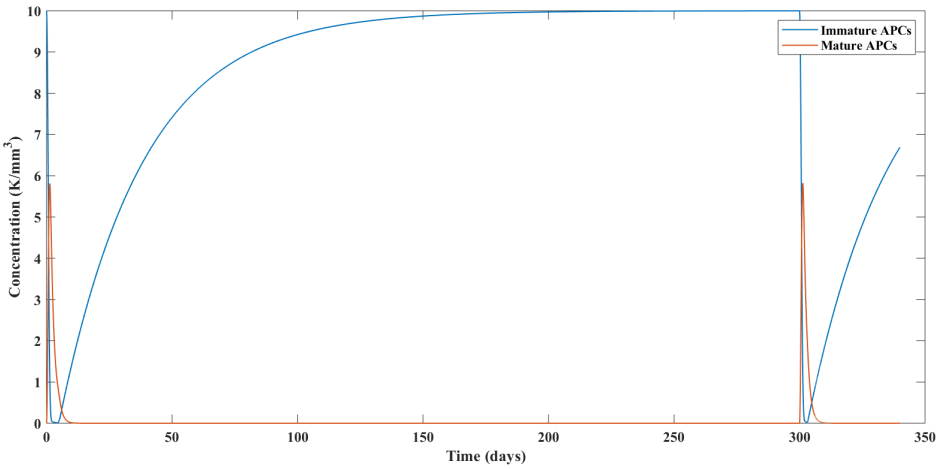

Figure 3.5: The dynamics of immature and mature APCs. Most of the dynamics don't change from primary immune response to the secondary immune response other than a reduced time to return to the initial population levels following the secondary response.

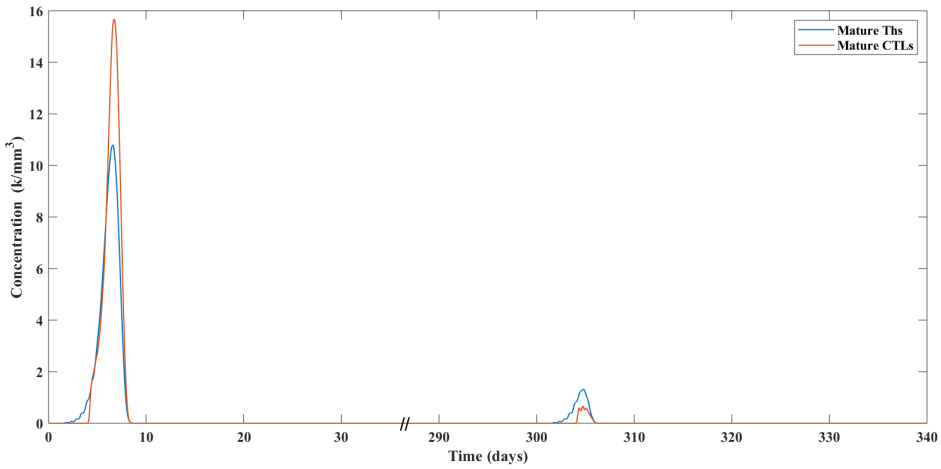

Figure 3.6: The dynamics of mature Ths and CTLs. We see a reduction in the amount of mature non-memory cells present in the secondary immune response in comparison to the primary immune response.

immune response, with primary antigen clearance around 6 days and secondary antigen clearance in around 3 days. Moreover, the maximum amount in the antigen concentration over the course of the secondary response is significantly lower than the peak of antigen concentration during the primary response.

Figures 3.6-3.8 show the evolution of the mature effector T cell and the memory T cell population concentration. Just as demonstrated experimentally, the dormant memory T cell population forms primarily during the contraction phase of the immune response. Moreover, when comparing the primary immune response to the secondary response, activated memory T cells dominate with far less non-memory effector T cells becoming activated. We see a slight increase in the amount of activated memory T cells after 25 days (shown in Figure 3.9). This slight increase in the amount of activated memory T cells is due to the fact that within our model, the concentration of mature APCs (shown in Figure 3.5) never reaches absolute zero.

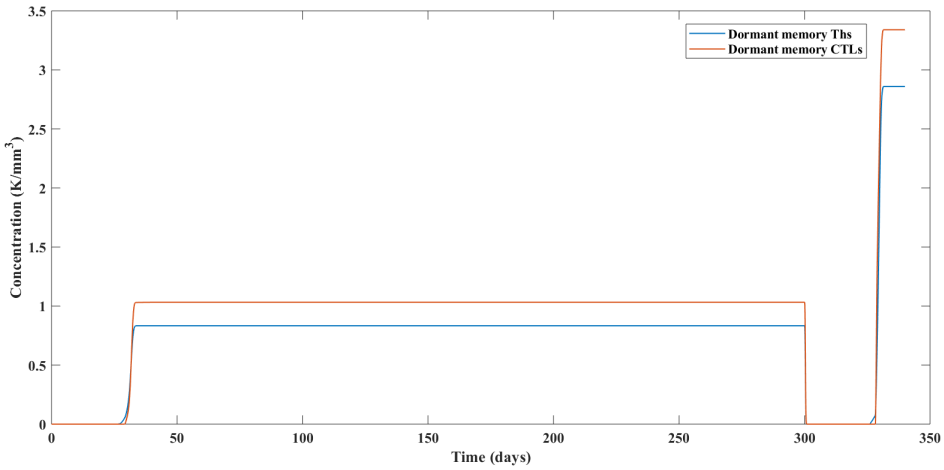

Figure 3.7: The dynamics of dormant memory Ths and CTLs. Memory cells are created and remain steadily at low levels—around 5-10% of the total amount of mature and activated cells during both immune responses.

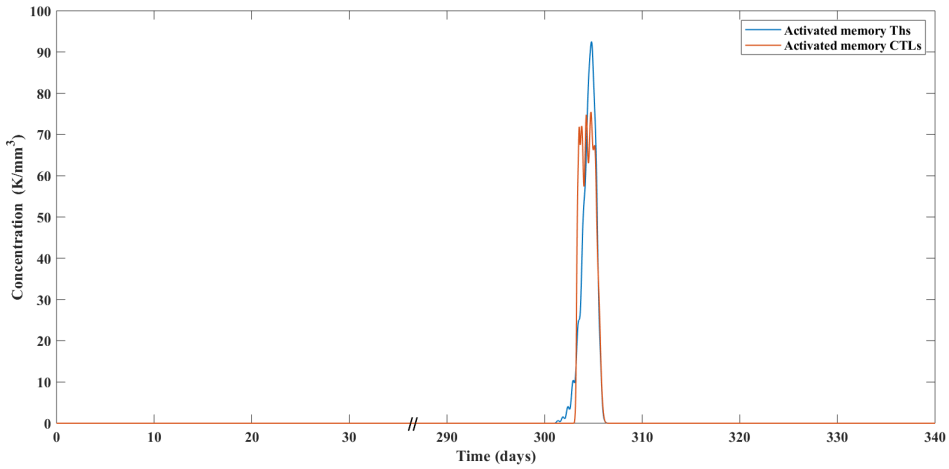

Figure 3.8: The dynamics of activated memory Ths and CTLs. We observe an increase in the activation speed and magnitude of the secondary response in comparison to the non-memory T cells in during the primary response.

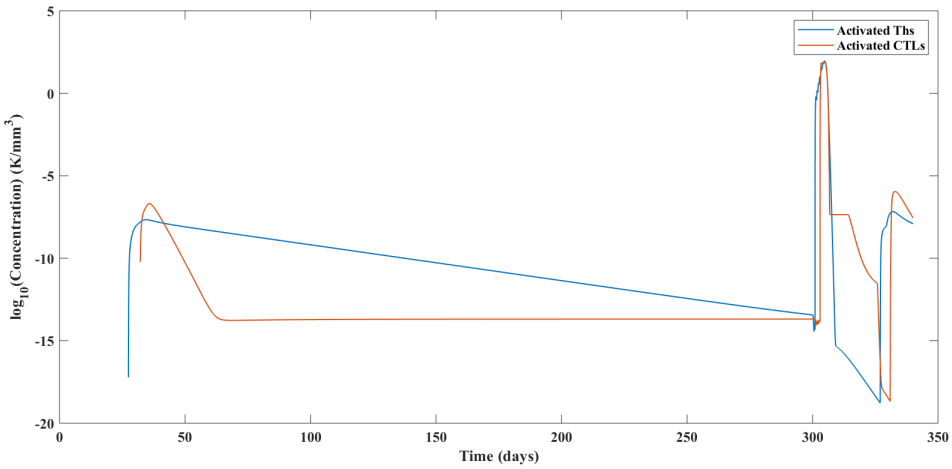

Figure 3.9: The $\log_{10}$ dynamics of activated memory Ths and CTLs. We observe a slight activation of memory T cells after day 25, due to the non-zero presence of antigen cells.

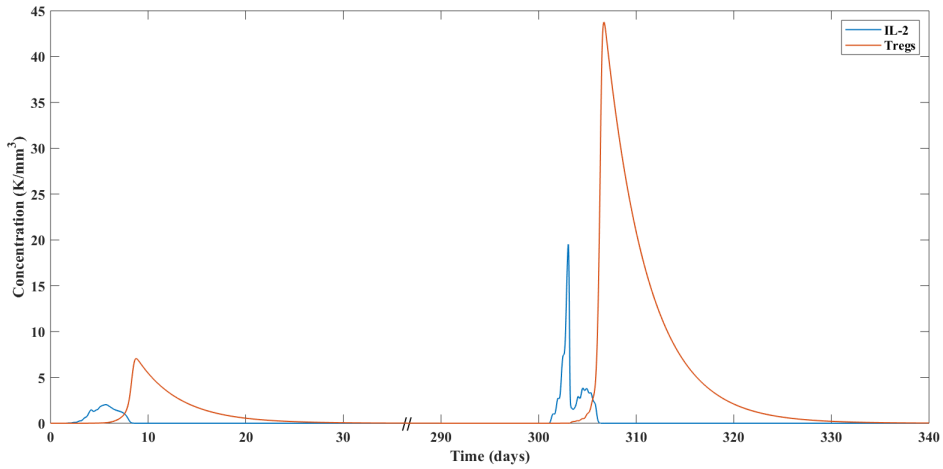

Figure 3.10: The dynamics of IL-2 and Tregs. We observe an increase in both the secretion of IL-2 and Tregs in the secondary immune response. These observations illustrate the 10% increase in IL-2 production of memory T cells and the increased regulation required for the contraction of the secondary immune response.

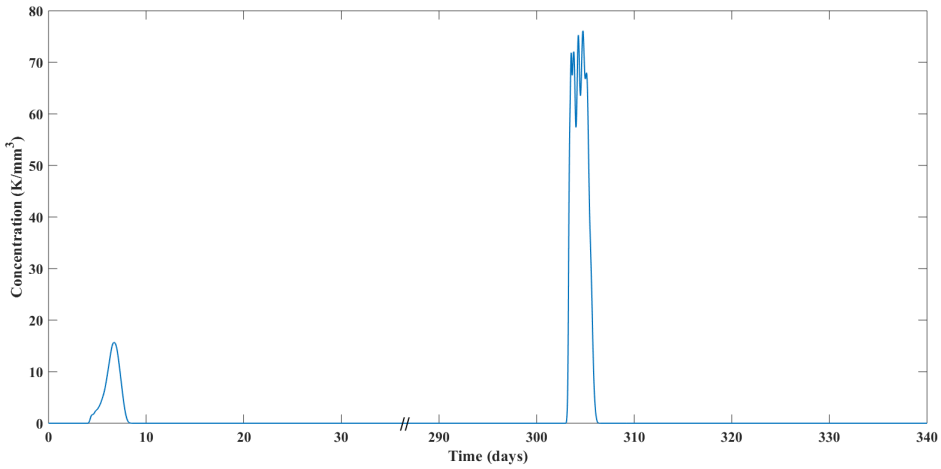

Figure 3.11: The dynamics of total CD8+T cells. Simulation results are similar to the observed data from Flynn et al. (1998) with the total amount of CD8+ T cells increasing 5 fold.

Though the difference in the evolution of APCs between primary and secondary immune responses (shown in Figure 3.5) is negligible, the amount of IL-2 and the number of Tregs that are created during the secondary response are significantly higher, see 3.10. This increase in IL-2 and Tregs is in direct response to the increase of the amount of activated memory T cells in the system. These memory T cells create more IL-2 and at the same time require more regulation than the mature effector T cells during the primary immune response. Similar to the activated memory T cells, there is an increase followed by a decrease in the amount of IL-2 in the system after 90 days. This increase is expected given that IL-2 is secreted by the small amount of activated memory T cells.

When comparing with the data found in Figure 3.3 from Flynn et al. (1998), we observe similar results in our simulation (Figure 3.11). There is a 5-fold increase in the total number of CD8+ T cells and faster activation during the secondary immune response in comparison to the primary response. We do not, however,

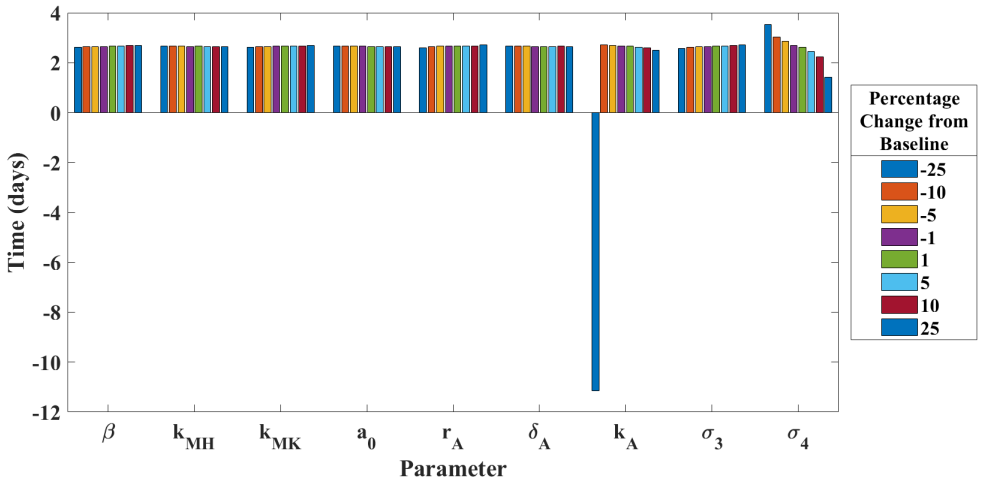

Figure 3.12: Sensitivity analysis of parameters for memory and antigen cell compartments. We compare the difference in time of antigen clearance between primary and secondary infection.

capture the amount of time that these CD8+ T cells sustain over time. The data indicates that is should take over 13 days to full contraction reduce, while our model has full contraction in less than 10 days for both responses [43].

3.3.1 Parameter Analysis

When testing the robustness of the parameters in our model, we compare the amount of time required to clear a primary infection, time = 0 days, with the amount of time required to clear a secondary infection, beginning at time = 70 days. Here, we vary each parameter centered around a baseline value. As seen in Figure 3.12 the majority of the parameters guiding the memory T cell and antigen compartments do not significantly change the clearance time of the secondary infection when varied from the baseline. The main parameter that affects the results with slight perturbation is the delay, σ_4, required for dormant killer cells to mature. As

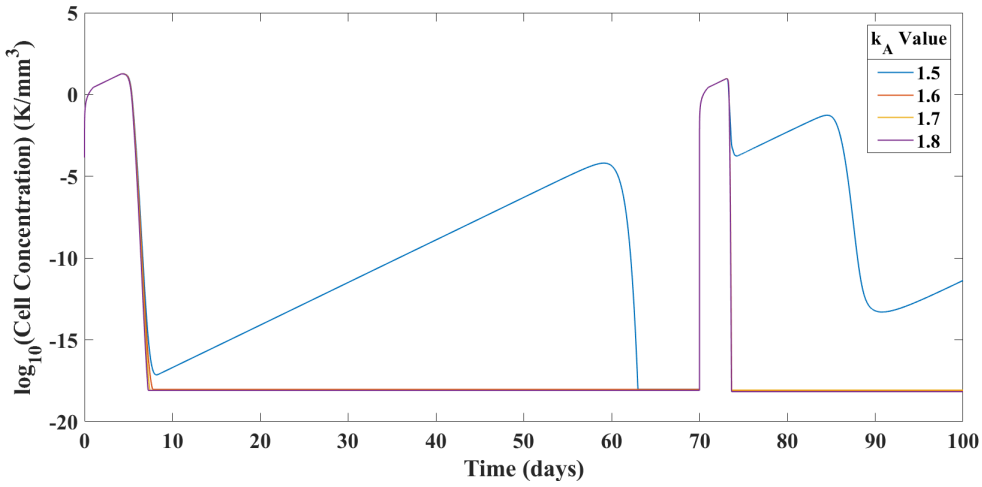

Figure 3.13: The dynamics of antigen cell concentrations with varying values of CTL-antigen kinetic coefficient k_A. We observe that once k_A reaches below 1.6, the concentration of antigen does not reach the threshold, 10^{-18}, required by the Heaviside equation in Equation 3.13 to prevent change in the antigen compartment.

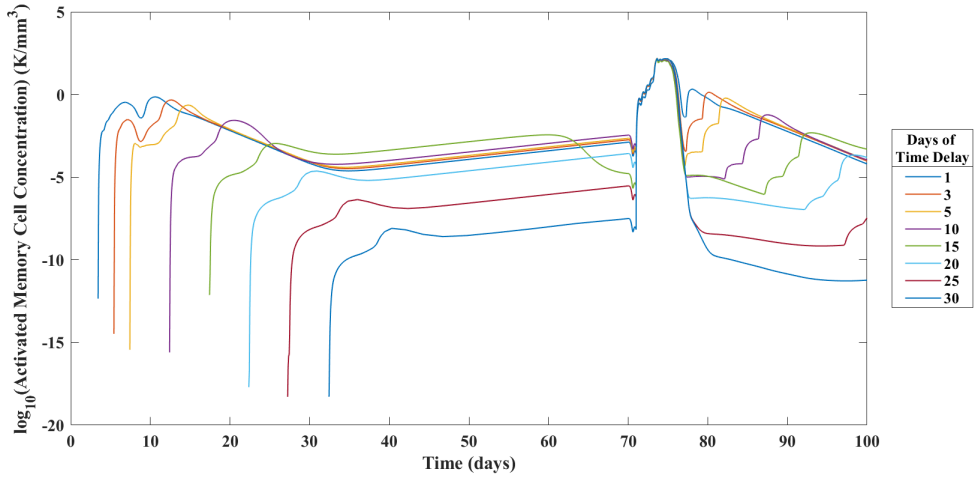

Figure 3.14: The dynamics of total activated memory T cells with varying delays in transition to dormant memory T cells, α. We do not observe a significant change in the activation of dormant memory cells after 25 days.

shown, the difference in the length of time of antigen clearance decreases with an increased amount of time required to mature. Thus, as expected by slightly lowering the time required for the mature memory T cells to become active, the clearance of antigen in a secondary infection happens more rapidly than in primary infection.

Contrastingly, when varying two parameters significantly, k_A and α, we see more of a change in the simulated results. Given that k_A is the kinetic coefficient for the CTL-antigen interaction, though performing similarly as the other parameter for the majority of changes from the baseline, once the parameter is lowered significantly, the time necessary to clear the secondary infection increases significantly. When varying k_A, we observe that once k_A reaches below around 1.6, the clearance of antigen from the primary infection does not reach below the 10^{-18} threshold required by the Heaviside equation in Equation (3.13) to prevent a change in the antigen compartment. See Figure 3.13.

The final parameter we observe is the parameter which governs the delay from when a mature effector T cell becomes a dormant memory T cell. The choice of α is done in order to prevent dormant memory T cells from being activated during the response period when they are created. This choice is driven by the assumption that though our model creates dormant memory T cells throughout the entire immune response, in nature the majority of dormant memory T cells are created at the end of the immune response. As seen in Figure 3.14, if we select the α at five days or below, the dormant memory cells become activated within the producing infection. Given that our system has residual IL-2 and antigen cells post immune response, the dormant memory cells become activated between infections. However,

the choice of twenty days guarantees that these activated memory cells remain in relatively low levels while ensuring that they will be available for activation for a subsequent infection within a reasonable timespan.

3.4 Discussion

During the construction of this model, we ran into some challenges. First, since we want effector T cells to convert into memory T cells based on a decrease of IL-2 in the system, though in small numbers, dormant memory T cells are created throughout the entire primary immune response. Moreover, since dormant memory T cells are activated by antigen presenting cells, if we allow dormant memory T cells to have the ability to activate too soon after conversion from effector T cells, APCs then have the ability to activate dormant memory cells throughout the primary immune response as well. Considering that it is unknown if memory T cells are immediately functional, even during a primary response, we assume that even though dormant memory cells are created throughout an immune response, there is a delay in the amount of time from conversion from effector T cells to having the ability to activate into functioning memory T cells. Given that our primary immune response lasts for roughly ten days, we make this delay in the ability to activate, α, twenty-five days. However, due to the continuous nature of our model, we still observe this activation of memory T cells in our simulations.

Another issue was the difficulty in getting populations in our model to go extinct in the mathematical model. For example, *in vivo*, it is safe to assume that

at the end of an immune response the amount ot antigen in the system is zero, i.e., all of the antigen cells have been eliminated. However, given that we are working with a system of differential equations, though populations may drop to very low values, these low levels can still activate the rest of the system. In our model, the antigen compartment is assumed to grow exponentially, so without the population at zero, it can still activate the APCs and activate the full cascade of an immune response. We address this issue by incorporating the Heaviside equation into the equation governing the kinetics of the antigen cell compartment. If the concentration of antigen cells drops below 10^{-18}, this added term makes the change in the antigen cells to go to zero. Though this does not fully stop the immune system from being activated, the amount of activation simulated by our mathematical model becomes negligible.

Other versions of this model were tested with differing characteristics of memory cells. As discussed earlier, by simply extending the model of Kim et al. (2010) to a secondary immune response, we see almost identical behavior to the primary response—no increase in IL-2 or speed in antigen clearance. This gave rise to adding a memory T cell compartment. As mentioned earlier, there is evidence of multiple subpopulations of memory T cells, central and effector—both captured in our model—as well as virtual and tissue resident memory T cells. Though it is possible to formulate more complex models with varying degrees of detail within T cell memory formation and activation, we observe that having one population of memory T cells for both CD4+ and CD8+ cells results in the overall dynamics desired. While there is more insight to be gained by expanding the memory T cell compartment to

more subpopulations, our aim was to observe how memory T cells play an overall role in antigen clearance as well as capture key features of memory T cell activation and expansion, which was accomplished.

Even though our model simulation does not mimic the full behavior of the antigen observed in Flynn et al. (1998), we maintain that our model is easily adaptable to parameter changes for any said antigen, both viral and bacterial. Through our parameter analysis, we observed that the behavior of the overall system is robust despite large perturbations in the majority of the memory T cell parameters.

3.5 Conclusion

Adaptive immunity in both primary and secondary immune responses encompasses a complex system of cells and cytokines that allow for both recognition and response to many antigens. In Sect. 3.2 we derived a DDE mathematical model to describe these dynamical interactions. We demonstrated that the model displays the expected dynamics of creating memory T cells during the contraction phase of an immune response and the expansion and contraction of the immune system during a secondary encounter with an antigen. More so than the creation of memory cells, we observe their use once activated and show that memory T cells are the main contributor to the elimination of antigen in secondary immune system activation.

The model presented does, however, only observe the immune system over two encounters with the same antigen. It can be extended to study the immune system over longer periods of time with multiple encounters with the same antigen, for

example with chronic diseases or autoimmunity. Given that there may be evidence of differing types of regulation for effector T cells and memory T cells, one can expand this model to capture the differences in the contraction of memory T cells and non-memory T cells. Further studies on the expansion and contraction of memory T cells can lead to models tackling questions surrounding vaccines and other immune stimulatory processes that create memory cells.

This work was carried out in collaboration with Grégoire Altan-Bonnet (ImmunoDynamics Group NIH/NCI).

Chapter 4: Immune-Induced Breast Cancer Dormancy

4.1 Overview

In the process of studying the progression and treatment of breast cancers, we find that a main tenant of poor prognosis amongst breast cancer patients is linked to secondary tumor sites. Specifically, within all breast cancer patients, 20-50% will develop metastatic breast cancer which has a 5-year survival of only 26% [44]. Therapies for primary lesions fair well in, and in many cancers result in remission. A relapse may occur after varying lengths of latency periods depending on the type of breast cancer (see Figure 4.1). When observing this dormant phase of breast cancer, the phase between remission and relapse, it is necessary to understand both the location of the secondary tumor within the body and how evasive these disseminated breast cancer cells (BCCs) are. Given that the main secondary site for breast cancer is the bone marrow, we focus our study on breast cancer dormancy in the bone marrow niche.

In this chapter, we develop a mathematical model to study the dynamics of adaptive immune-induced breast cancer dormancy. Specifically, we aim to better understand the roles of memory T cells and regulatory T cells in he ability of BCCs to remain in low numbers for long periods of time. We develop our mathematical

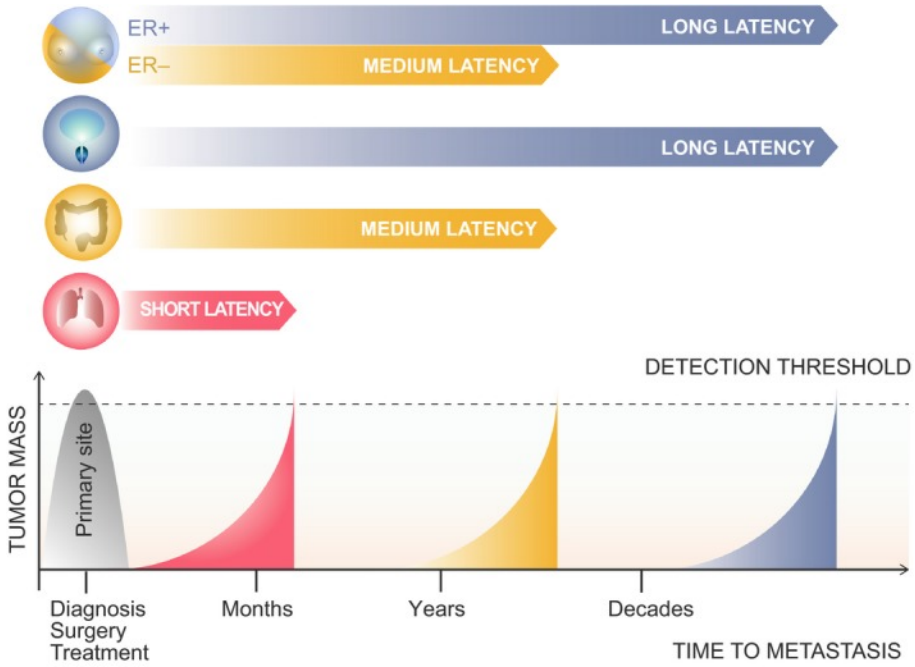

Figure 4.1: Representation of the varying latency periods of cancer types. Figure taken from Gomis and Gawrzak (2017) [14]. We observe that with breast cancer types ER- and ER+, there are medium and long latency periods, respectively, until relapse.

model by extending the adaptive immunity model of Chapter 3 to incorporate key biological features specific to BCCs that are disseminated to the bone marrow. These features are outlined below:

1. BCCs evade immune clearance by recruiting mesenchymal stem cells (MSCs) in the bone marrow.

2. MSCs produce TGF-β, which suppresses cytotoxic T cell function and increases the number of helper cells that transition to regulatory T cells (Tregs)

3. These Tregs actively suppress immune system function by increasing the amount of T cells that enter apoptosis.

We use the model to demonstrate that with the addition of immune suppression by

BCCs, BCCs have the ability to enter into a state of immune-induced dormancy with latency periods varying on the evasiveness of the breast cancer cells.

4.2 A Model for Breast Cancer Dormancy

Following the framework developed in Chapter 3, we develop a delayed differential equation model which includes breast cancer cells as the antigen compartment. We incorporate immunological factors specific to disseminated BCCs in the bone marrow. Our model is shown in Figure 4.2, and includes the following elements:

1. Immature APCs, $A_0(t)$, become mature APCs, $A_1(t)$ when they interact with breast cancer cells, $B(t)$. Mature APCs travel to the lymph nodes.

2. In the lymph nodes, the naïve helper T cells, $H^0(t)$, and naïve cytotoxic T cells, $K^0(t)$, interact with the mature APCs and begin to undergo the minimal developmental program. Here the helper T cells and the CTLs divide m_1 and m_2 times, respectively, for the duration of σ_1 and σ_2, respectively.

3. In primary immune response, during the contraction phase, when the amount of IL-2, $P(t)$, is low, mature helper T-cells and mature CTLs, transition into dormant memory helper cells, $M_H^0(t)$, and dormant memory CTLs, $M_K^0(t)$, respectively. In the contraction phase of secondary and subsequent immune responses, mature helper T cells and activated memory helper cells, $M_H(t)$, both transition to $M_H^0(t)$. Similarly, mature CTLs and activated memory CTLs, $M_K(t)$, both transition to $M_K^0(t)$ during the contraction phase of secondary and subsequent immune responses. The duration of the transition into

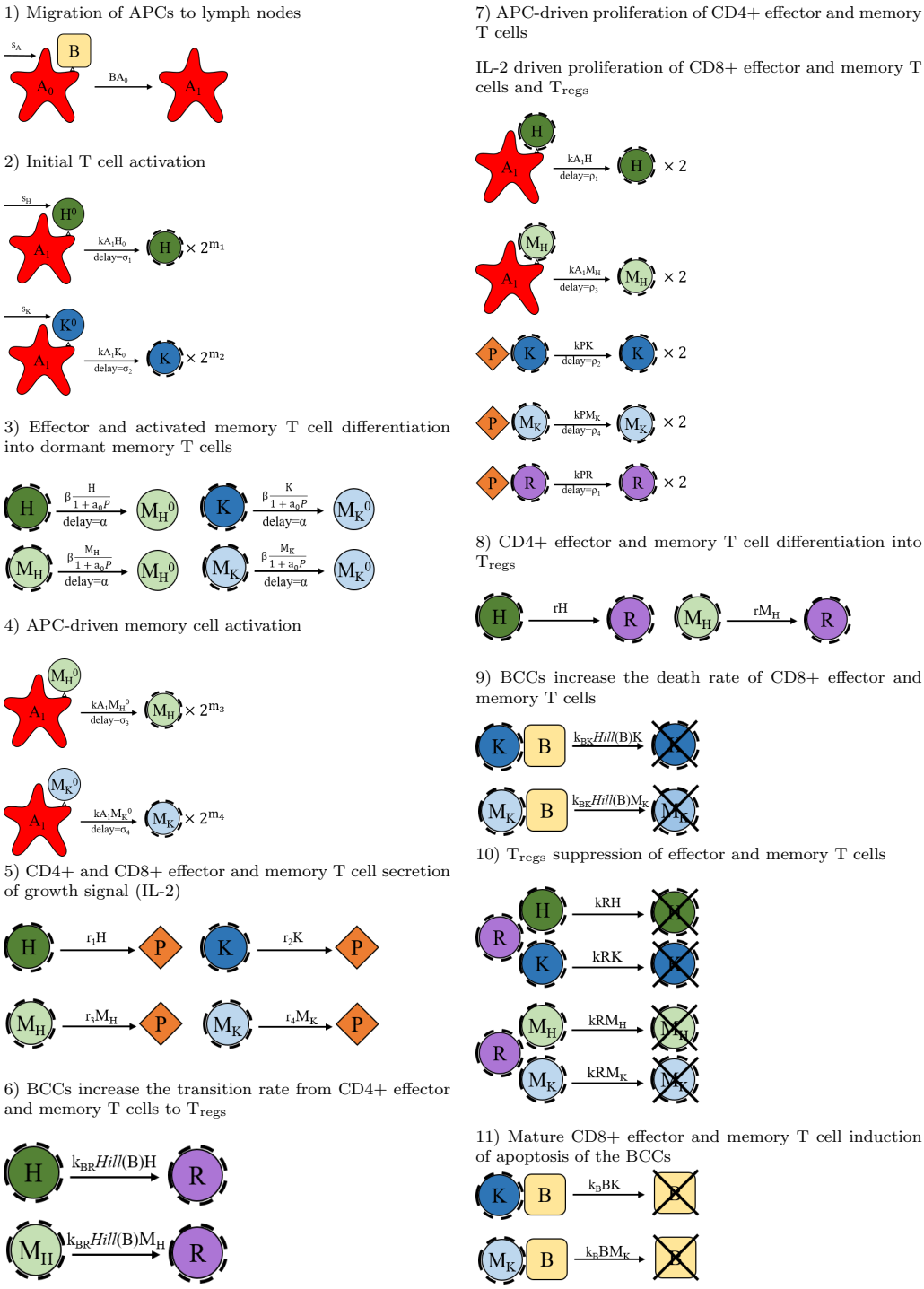

Figure 4.2: Diagram of the breast cancer dormancy model (4.1)-(4.13). The compartments are represented as follows: A_0: immature APCs, A_1: mature APCs, H^0: naïve helper T cells, H: mature helper T cells, K^0: naïve cytotoxic T cells, K: mature cytotoxic cells, M_H^0: dormant memory helper T cells, M_H: activated memory helper T cells, M_K^0: dormant memory cytotoxic T cells, M_K: activated memory cytotoxic cells, P: IL-2 concentration, R: regulatory T cells, and B: breast cancer cells.

$M_H^0(t)$ and $M_K^0(t)$ is α.

4. In secondary and subsequent immune responses, the dormant memory T cells, interact with mature APCs causing them begin the minimal developmental program. Here the memory helper T cells and the memory CTLs divide m_3 and m_4 times, respectively, for the duration of σ_3 and σ_4, respectively.

5. Both mature effector T cells and activated memory T cells secrete the growth signal IL-2, $P(t)$.

6. Disseminated BCCs increase the transition rate from both effector and memory helper T cells to regulatory T cells.

7. Once mature T cells and activated memory T cells complete the minimal developmental program, they become effector T cells and continue to divide. The CD4+ cells continue to proliferate in response to an interaction with the mature APCs, while CD8+ cells proliferate in response to stimulation by IL-2.

8. A proportion of mature helper T cells and activated memory helper cells transition into regulatory T cells in response to stimulation by BCCs.

9. Disseminated BCCs increase the death rate of both effector and memory CTLs.

10. Regulatory T cells suppress mature effector T cells as well as activated memory T cells. They also proliferate in response to IL-2 stimulation.

11. Mature CTLs and activated memory CTLs induce apoptosis in BCCs.

The model for adaptive immunity dynamics during breast cancer dormancy is given by the following equations:

$$\dot{A}_0 = s_A - d_0 A_0(t) - B(t)A_0(t), \tag{4.1}$$

$$\dot{A}_1 = B(t)A_0(t) - d_1 A_1(t), \tag{4.2}$$

$$\dot{H}^0 = s_H - \delta_0 H^0(t) - kA_1(t)H^0(t), \tag{4.3}$$

$$\begin{aligned}\dot{H} &= 2^{m_1} kA_1(t-\sigma_1)H^0(t-\sigma_1) - kA_1(t)H(t) + 2kA(t-\rho_1)H(t-\rho_1) \\ &\quad - (\delta_H + r)H(t) - kR(t)H(t) - \beta\frac{H(t)}{1+a_0P(t)} \\ &\quad - k_{BR}(Hill(q_2, B(t))H(t)),\end{aligned} \tag{4.4}$$

$$\dot{K}^0 = s_k - \delta_0 K^0(t) - kA_1(t)K^0(t), \tag{4.5}$$

$$\begin{aligned}\dot{K} &= 2^{m_2} kA_1(t-\sigma_2)K^0(t-\sigma_2) - kP(t)K(t) + 2kP(t-\rho_2)K(t-\rho_2) - \delta_k K(t) \\ &\quad - k_E R(t)K(t) - \beta\frac{K(t)}{1+a_0P(t)} - k_{BK}Hill(q_1, B(t))K(t),\end{aligned} \tag{4.6}$$

$$\begin{aligned}\dot{M}_H^0 &= \beta\frac{H(t-\alpha)}{1+a_0P(t-\alpha)} + \beta\frac{M_H(t-\alpha)}{1+a_0P(t-\alpha)} + (r_{MH} - \delta_{MH})M_H^0(t) \\ &\quad - k_{MH}A_1(t)M_H^0(t),\end{aligned} \tag{4.7}$$

$$\begin{aligned}\dot{M}_H &= 2^{m_3} k_{MH}A_1(t-\sigma_3)M_H^0(t-\sigma_3) - kA_1(t)M_H(t) + 2kA_1(t-\rho_1)M_H(t-\rho_1) \\ &\quad - (\delta_H + r)M_H(t) - kR(t)M_H(t) - \beta\frac{M_H(t)}{1+a_0P(t)} \\ &\quad - k_{BR}(Hill(q_2, B(t))M_H(t)),\end{aligned} \tag{4.8}$$

$$\begin{aligned}\dot{M}_K^0 &= \beta\frac{K(t-\alpha)}{1+a_0P(t-\alpha)} + \beta\frac{M_K(t-\alpha)}{1+a_0P(t-\alpha)} + (r_{MK} - \delta_{MK})M_K^0(t) \\ &\quad - k_{MK}A_1(t)M_K^0(t),\end{aligned} \tag{4.9}$$

$$\dot{M}_K = 2^{m_4} k_{MK}A_1(t-\sigma_4)M_K^0(t-\sigma_4) - kP(t)M_K(t) + 2kP(t-\rho_2)M_K(t-\rho_2)$$

$$- \delta_k M_K(t) - k_E R(t) M_K(t) - k_{BK} Hill(q_1, B(t)) M_K(t) - \beta \frac{M_K(t)}{1 + a_0 P(t)}, \tag{4.10}$$

$$\dot{P} = r_1 H(t) + r_2 K(t) + r_3 M_H(t) + r_4 M_K(t) - \delta_P P(t)$$

$$- kP(t)K(t) - kP(t)M_K(t) - kP(t)R(t), \tag{4.11}$$

$$\dot{R} = r(H(t) + M_H(t)) + 2kP(t - \rho_1)R(t - \rho_1) - kP(t)R(t) - \delta_H R(t)$$

$$+ k_{BR}(Hill(q_2, B(t))H(t) + Hill(q_2, B(t))M_H(t)), \tag{4.12}$$

$$\dot{B} = [(r_B - \delta_B)B(t) - k_B(B(t)K(t) - B(t)M_K(t))] \times \theta(B(t) - 10^{-18}), \tag{4.13}$$

where,

$$Hill(q, B(t)) = \frac{B^3(t)}{q^3 + B^3(t)}. \tag{4.14}$$

A_0 represents the concentration of immature APCs at the site of infection, while A_1 is the concentration of mature APCs that are presenting antigen in the lymph nodes. H^0 represents the concentration of naïve helper T cells and H is the concentration of mature helper T cells. Similarly, K^0 and K represent the concentration of immature and mature cytotoxic T cells, respectively. M_H^0 and M_H represent the concentration of dormant and activated memory helper T cells, while M_K^0 and M_K represent the concentration of dormant and activated memory cytotoxic T cells. Finally, P represents interleukin-2 concentration, R represents regulatory T cell concentration, and B represents BCC concentration.

Equation (4.1) describes the immature APCs that are available in the body to respond to breast cancer cell stimulation. We assume is a constant supply rate of the cells, s_A, and a death rate, d_0, that is proportionate to the amount of immature APCs. Immature APCs are stimulated by the amount of BCCs in the system, B, and through this stimulation immature APCs become the mature APCs in the lymph nodes described by (4.2). Mature APCs also have a death rate proportional to the amount of mature APCs in the system, d_1.

Equations (4.3) and (4.5) describe naïve T cell populations for helper T cells and cytotoxic T cells, respectively. Both populations have constant supply rates, s_H and s_K, and a death rate, δ_0, that is proportional to the amount of each of the naïve T cell populations. These naïve T cells transition into their respective effector T cell populations based on the mass action interaction with mature APCs.

The mature helper T cell population is described by Equation (4.4). After the naïve CD4+ cells become activated by mature APCs, the first term shows the rate at which they enter the minimal developmental program where they undergo m_1 cell divisions. The amount of time required for this developmental program is characterized by the time delay σ_1. Once the cells are fully mature, CD4+ cells are further stimulated by APCs and proliferate, the rate at which this division occurs is shown by the second and third terms. The amount of time required for a mature helper T cells to divide is represented by the time delay ρ_1.

Mature helper T cells are removed from the system by either natural cell death, δ_H, differentiation into regulatory T cells, r, regulatory T cells suppression, or differentiation into dormant memory cells. Since we assume that dormant memory

cells are formed during the contraction phase of immune response, the last term shows the rate of CD4+ cells switching to dormant memory cells occurring when the amount of IL-2 is low. The final term accounts for the increase in the amount of helper T cells that transition to regulatory T cells due to the amount of BCCs in the system.

Equation (4.6) describes the mature cytotoxic T cell population. Similar to the mature helper T cells, the first term shows the rate at which naïve CD8+ cells enter the mature cell population after undergoing the minimal developmental program of m_2 cell divisions. The amount of time required for this developmental is given by the time delay of ρ_2. Further proliferation of CD8+ cells is activated by IL-2, the second and third terms, with the duration of one cell division of CD8+ cells shown by the time delay ρ_2. CD8+ cells exit the system by either natural cell death, δ_K, suppression by regulatory T cells, or by differentiating into dormant memory CTLs when the amount of IL-2 is low, or during the contraction phase. They also will exit the system due to increased numbers of BCCs.

Equations (4.7) and (4.9) describe the dormant helper and CTL memory cells, respectively. The first two terms of each equation show the rates at which cells are transitioning from either their respective mature T cell populations or their respective activated memory T cell compartment. We assume that after transition from the effector T cell compartments, dormant memory T cells can be activated only after a time (α) passes. The third terms describe the proportionate growth rate, r_{M*}, and natural death rate, δ_{M*}. The final terms describe the rates at which dormant cells become activated. Similar to naïve T cells, dormant memory cells

become activated based on the mass action interaction with mature APCs.

The activated memory T cell populations are described by Equations (4.8) and (4.10), representing CD4+ and CD8+ T cells, respectively. Similar to the activation of non-memory T cells, after the dormant memory cells become activated by mature APCs, the first term shows the rate at which they enter the minimal developmental program where they undergo m_3 and m_4 cell divisions. The amount of time required for this developmental program is characterized by the time delays σ_3 and σ_4. Once the cells are fully activated, CD4+ cells are further stimulated by APCs and proliferate, while CD8+ cells are further stimulated by IL-2. The amount of time required for activated memory CD4+ and CD8+ T cells to divide is represented by the time delays ρ_1 and ρ_2, respectively.

Activated memory CD4+ T cells are removed from the system by either natural cell death, δ_H, differentiation into regulatory T cells, r, regulatory T cells suppression, or differentiation into dormant memory cells. Moreover, activated memory CD4+ T cells also have an additional transition to regulatory T cells proportionate to the amount of BCCs in the system. In contrast, activated memory CD8+ T cells are removed from the system by either natural cell death, δ_K, regulatory T cells suppression, or differentiation into dormant memory cells. They are removed from the system based on the number of BCCs in the system. Since we assume that dormant memory cells are formed during the contraction phase of an immune response, the last term of both equations shows the rate of activated memory cells switching to dormant memory cells which occurs when the amount of IL-2 is low.

Equation (4.11) describes the amount of IL-2 in the system. The first four terms show the rate at which IL-2 is secreted by mature helper t cells (r_1), mature CTLs (r_2), activated memory helper T cells (r_3), and activated memory CTLs (r_4). The cytokine has a decay rate, δ_P, proportionate to its amount. IL-2 is also consumed by mature CTLs, activated memory CTLs, and Tregs, given by the last three terms.

The dynamics of regulatory T cells is governed by equation (4.12). The first term gives the rate at which mature helper T cells and activated memory T cells differentiate into Tregs. The next two terms describe the rate at which Tregs further proliferate based on IL-2 activation, with the duration of one Treg cells division characterized by the time delay ρ_1. Next, Tregs exiting the system by the same natural death rate of helper T cells, δ_H. Finally, the last term represents the additional CD4+ T cells that transition from the non-memory and memory T cell compartments due to the amount of BCCs in the system.

The final equation, (4.13), describes the dynamics of the breast cancer cells. The first term describes their proportionate growth rate, r_B, and death rate, δ_B. BCCs are removed from the system via interaction with mature CTLs and activated memory CTLs, the second and third term, respectively. Finally, $\theta(t)$ is the Heaviside equation, with

$$\theta(t) = \begin{cases} 0 & t < 0, \\ \frac{1}{2} & t = 0, \\ 1 & t > 0. \end{cases}$$

Here, the Heaviside equation prevents the breast cancer cells from changing once its population falls below a threshold which we set as 10^{-18} K/mm^3. Consequently, this addition reduces the amount of consistent stimulation of the immune cells in the model.

4.3 Numerical Results

Using the parameter values shown in Table 4.1 we solve Eqs. (4.1)-(4.13) numerically. All simulations were carried out using the MATLAB solver DDESD and the cell concentrations are measured in thousands of cells per cubic mm of blood (K/mm^3). The majority of the parameters used the values found in Kim et al. (2010) and Wilson et al. (2013) [22,40]. We allow for the system to run for 1000 days and assumptions that are made for these simulations are as follows:

1. We assume that the breast cancer cells are initially in sufficiently low enough levels that the immune system can fight the infection.

2. Both memory and non-memory CD8+ T cells act on breast cancer cells at the same rate.

3. Breast cancer cells activate the immune system in the same way an acute infection activates the immune system through constant stimulation.

4. We aim to represent early stage breast cancer dormancy and assume that amount of T cell exhaustion is negligible.

Parameter	Description	Estimate	Source
$A_0(0)$	Initial concentration of immature APCs	10	Kim
$H_0(0)$	Initial concentration of naïve CD4+ T cells	0.06	Kim
$K_0(0)$	Initial concentration of naïve CD8+ T cells	0.04	Kim
$B(0)$	Initial concentration of breast cancer cells	0.001	estimated
s_A	Supply rate of immature APCs	0.3	Kim
d_0	Death rate of immature APCs	0.03	Kim
d_1	Death rate of mature APCs	0.8	Kim
s_H, s_K	Supply rate of naïve CD4+ and CD8+ T cells, respectively.	0.0018, 0.0012	Wilson
k	Kinetic coefficient	5	Wilson
δ_0	Death rate of naïve T cells	0.03	Wilson
δ_H, δ_K	Death rate of mature CD4+ and CD8+ T cells, respectively.	0.23, 0.4	Wilson
m_1, m_2	Number of divisions in the minimal developmental program for naïve CD4+ and CD8+ T cells, respectively.	2, 7	Wilson
σ_1, σ_2	Duration of the minimal developmental program for naïve CD4+ and CD8+ T cells, respectively.	1.46, 4	Wilson
ρ_H, ρ_K	Duration of one T cell division for mature CD4+ and CD8+ T cells, respectively	11/24, 1/3	Wilson
k_E	Kinetic coefficient for CTL-Treg interactions	20	Wilson
β	Rate of differentiation of mature effector T cells into dormant memory effector T cells	0.3	estimated
α	Duration of time for cells to switch into dormant memory effector T cells	20	estimated
r_{MH}, r_{MK}	Growth rate of dormant memory CD4+ and CD8+ T cells, respectively.	0, 0	assumed
δ_{MH}, δ_{MK}	Death rate of dormant memory CD4+ and CD8+ T cells, respectively.	0, 0	assumed
k_{MH}, k_{MK}	Kinetic coefficient for mature APC-memory T cell interactions	5, 5	estimated
m_3, m_4	Number of divisions in the minimal developmental program for dormant memory CD4+ and CD8+ T cells, respectively.	3, 8	estimated
σ_3, σ_4	Duration of the minimal developmental program for dormant memory CD4+ and CD8+ T cells, respectively.	1, 3	estimated
a_0	Magnitude of dependence of dormant memory T cell differentiation on IL-2	5	estimated
r_1, r_2	Rate of IL-2 secretion by mature CD4+ and CD8+ T cells, respectively	10, 1	Kim
r_3, r_4	Rate of IL-2 secretion by activated memory CD4+ and CD8+ T cells, respectively	12.3, 3.3	estimated
δ_P	Decay rate of free IL-2	5.5	Wilson
r	Rate of differentiation of mature and activated memory CD4+ T cells into regulatory T cells	10	estimated
k_{BR}	Rate of differentiation of CD4+ T cells into Tregs due to BCCs	40	estimated
k_{BK}	Rate of decreased number of CD8+ T cells due to BCCs	40	estimated
r_B	Growth rate of breast cancer cells	0.06	estimated
δ_B	Death rate of breast cancer cells	0.04	estimated
k_B	Kinetic coefficient for CTL-antigen interactions	0.068	estimated
q_1, q_2	Hill function half maximum points	0.004, 0.004	estimated

Table 4.1: Estimates of parameters for model (4.1)-(4.14). All concentrations are measured in K/mm^3 and time is in days. Initial conditions not provided in the table are zero.

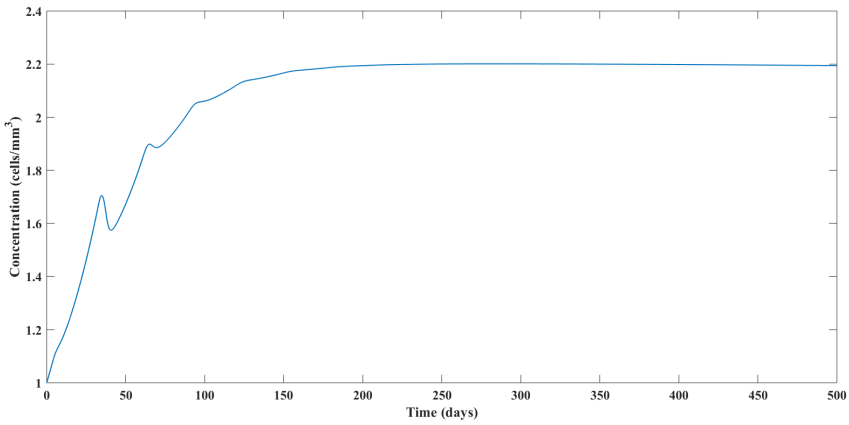

Figure 4.3: The dynamics of breast cancer cell concentration. After an initial increase and decrease of the breast cancer cell population, we see BCCs a slight oscillatory behavior until the dynamics level out at around 2.2 cells/mm^3 cells. This amount is below detection level, but the amount is sufficient for causing immune system stimulation.

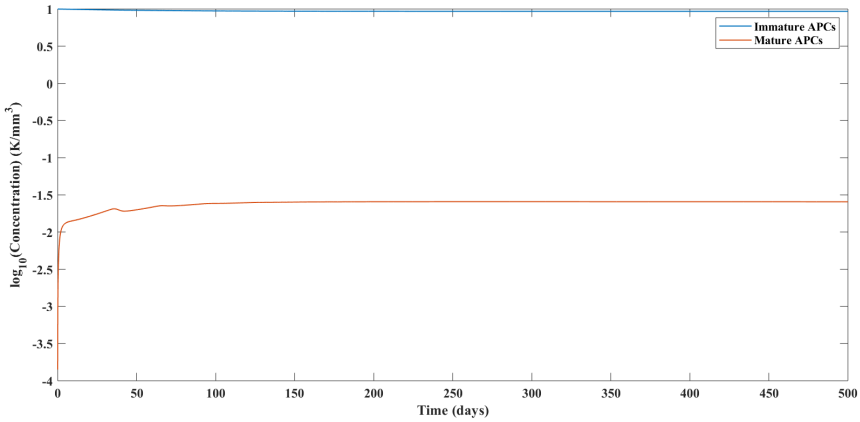

Figure 4.4: The dynamics of immature and mature APCs. Given the low levels of BCCs and the slow growth rate, we see minimal activation of APCs with sustained levels at about 0.03 K/mm^3 cells.

Figure 4.3 shows the concentration of breast cancer cells over a 500 days. We observe that after the initial growth and reduction of BCCs by the immune system, the cells rise and remain at low levels around 2.2 cells/ mm^3. Though a small number of cells, this dormant state causes oscillatory behavior that corresponds to the activation and contraction of the immune cells. Specifically, we see a small activation of the antigen presenting cells (Figure 4.4). While also in small numbers, we observe immature APCs converting over to mature APCs when there is a rise in the breast cancer cell concentration.

Figures 4.5 and 4.6 we show the concentrations of IL-2, regulatory T cell, and non-memory T cells. In response to the dynamics of the mature APCs, we observe similar results to those of a primary immune response during an acute infection. These dynamics are followed by low level constant behavior. Dormant memory T cell dynamics are shown in Figure 4.7. These cells are created after a delay of 25 days, and are sustained long term. While we see constant amounts of dormant memory helper T cells after day 250, we observe small increases in the amount of dormant memory CTLs over time. This increase is due to the fact that effector and activated memory T cells transition to the dormant memory compartment when the amount of IL-2 is low. Given the oscillatory dynamics of IL-2 early on, whenever the amount of IL-2 drops, we see an in increase in the dormant memory T cell compartment after 25 days.

Finally, the dynamics of the activated memory T cell compartment are shown in Figure 4.8. These cells activate with larger and faster immune dynamics similar to memory T cells responding to a secondary acute infection. However, due to the

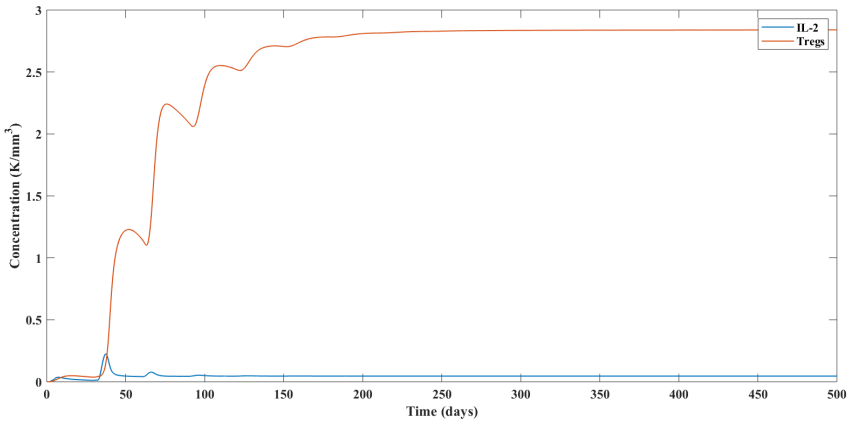

Figure 4.5: The dynamics of IL-2 and Tregs. The amount of IL-2 secreted as well as the amount of Tregs that are present mimic the amount and type of the activated T cells. They maintain low levels beginning with oscillatory behavior and leveling out around day 150.

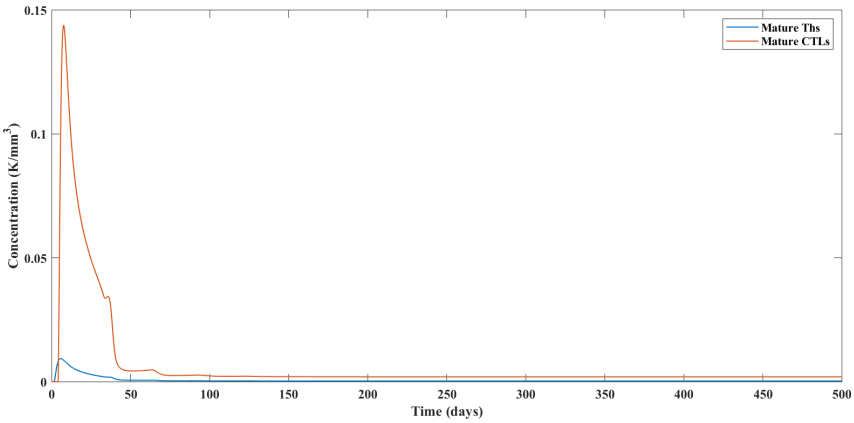

Figure 4.6: The dynamics of mature Ths and CTLs. Following initial immune activation, we see activation corresponding to the initial rise of the breast cancer cells. These cells are sustained at low levels following the initial response.

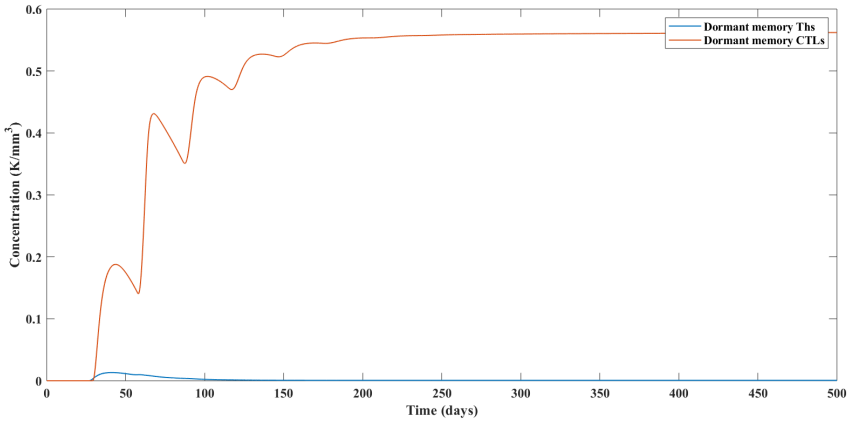

Figure 4.7: The dynamics of dormant memory T cells. A small immune activations results with small increases in the amount of dormant memory CTLs over time. This correlates with the early oscillatory behavior of IL-2, causing activated memory T cells to transition into the dormant compartment when IL-2 is low.

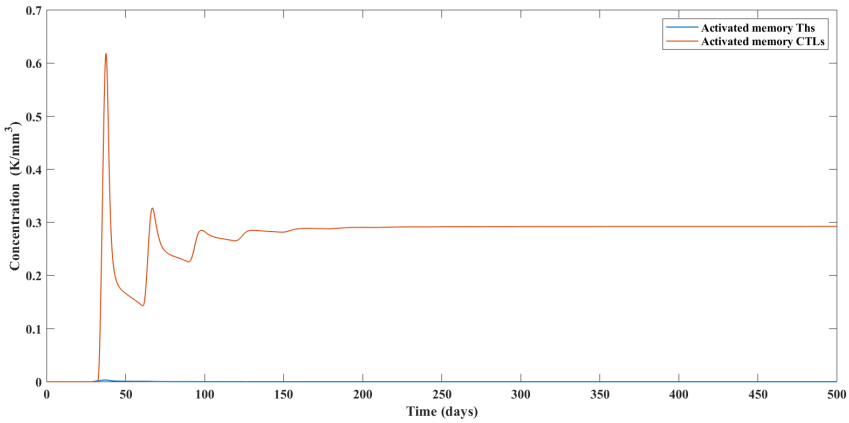

Figure 4.8: The dynamics of activated memory T cells. Prior to day 150, we see oscillatory behavior of memory T cells in low numbers proportional to the low levels of breast cancer cells. In comparison to the non-memory T cells, the total number of activated memory T cells is significantly greater.

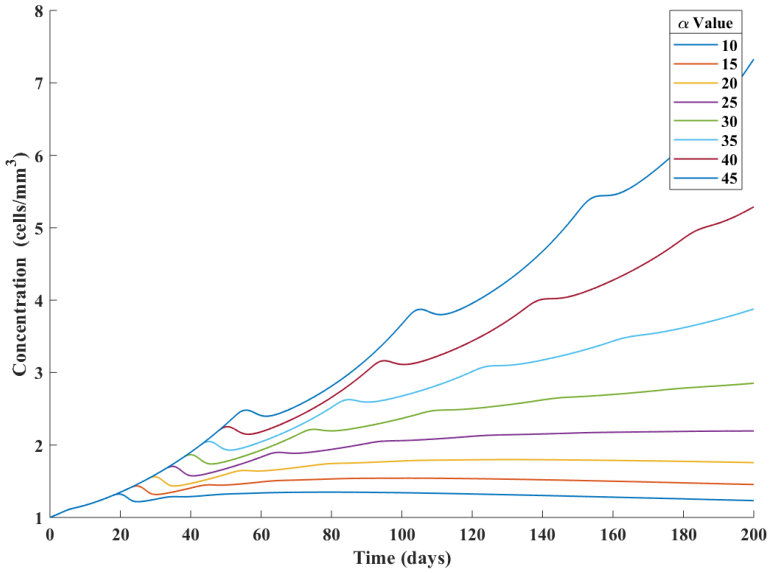

Figure 4.9: Sensitivity analysis of parameter, α. We see that with a shorter delay in the transition to dormant memory T cells, BCCs are more likely to remain at a dormant level. With a longer delay, we see a BCCs continuously growing.

immune suppression by the breast cancer cell compartment, the T cells are unable to fully eliminate the breast cancer cell population. Thus, there is constant immune system stimulation causing the activated memory T cells to display an oscillatory behavior early on, leveling out at 0.3 K/mm^3 cells after day 150. In contrast to the non-memory T cells, the activated memory T cells are maintained at a higher level. Specifically, there is shown to be a one to two orders of magnitude difference between the concentration levels of the non-memory and the memory T cells.

4.3.1 Parameter Analysis

In order to test the robustness of our model, we performed parameter analysis of the breast cancer cell concentration parameters (see Figures 4.9-4.12). We vary each parameter in a range of ±25% centered around the baseline values found in

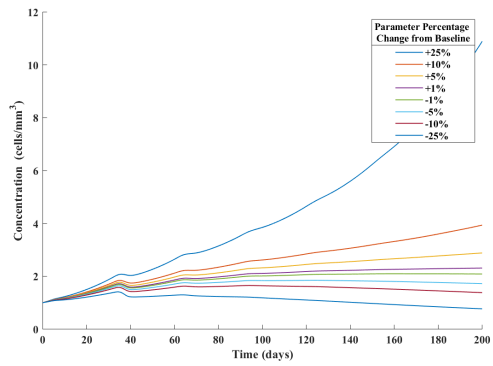

(a) Sensitivity analysis of parameters, $r_B - \delta_B$

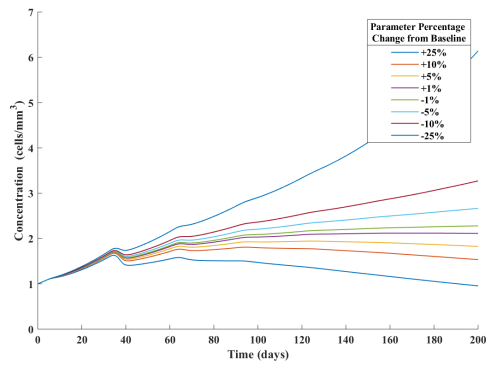

(b) Sensitivity analysis of parameter, k_B

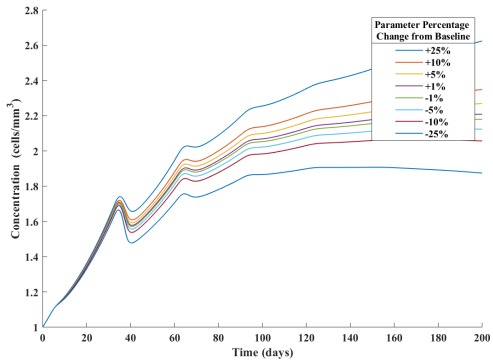

(c) Sensitivity analysis of parameters, k_{BK}

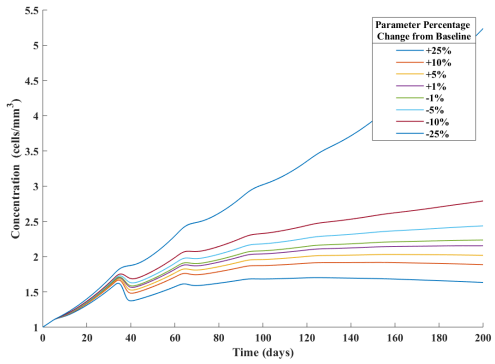

(d) Sensitivity analysis of parameter, q_1

Figure 4.10: Sensitivity analysis of parameters: $r_B - \delta_B$, k_B, k_{BK}, and q_1. Here, $r_B - \delta_B$ is the overall growth and death rate of the breast cancer cells, k_B is the rate at which CTLs eliminate the BCCs, k_{BK} represents the rate of reduction of CTL function due to breast cancer cells, and q_1 is the Hill function half maximum point for this reduction in CTL function. We observe that with large changes in all parameters, we see a significant change in the outcome of breast cancer dormancy. Namely, with larger values of $r_B - \delta_B$ and k_{BK} and smaller values of k_B and q_1, we observe long term growth of BCCs. Varying the parameters in the opposite direction, we see long term contraction of BCCs.

Table 4.1 and observe the final outcome of the breast cancer cells. In some fluctuations of the parameters, we still observe the breast cancer cells entering into a state of dormancy. Moreover, we do find that some parameters alter the levels of the final dormant state more than others.

The first parameter value analyzed is the memory T cell transition delay, α (Figure 4.9). We analyzed this term due to the fact that the final chosen value of α is arbitrary. We observe that the main consequence of fluctuating this delay is a change in whether or not the breast cancer cells enter a dormant state. With short transitions delays, $\leq$25 days, we see the BCCs entering into a state of dormancy. Longer transition delays result in long term BCC growth. This result follows from the fact that following initial immune activation, memory T cells are shown to be the primary effector T cells acting in subsequent immune responses. So, if the delay to transition is short, we see immune activation happening sooner than if we implement a longer transition delay.

When we fluctuate the majority of the breast cancer cell parameters, $r_B - \delta_B$, k_B, k_{BK}, and q_1, we observe significant changes in the final dormant level of the BCCs (see Figure 4.10). In particular, we see that with small changes in these parameters, the BCCs go into a state of dormancy. However, with larger fluctuations in the parameter values we observe the following. With larger values of $r_B - \delta_B$ and k_{BK} and smaller values of k_B and q_1, we observe long term growth of BCCs. However, with smaller values of $r_B - \delta_B$ and k_{BK} and larger values of k_B and q_1, we see long term contraction of BCCs. Given that an increase in $r_B - \delta_B$ and k_{BK} and a decrease in k_B and q_1 correspond with more aggressive breast cancer cells, the final

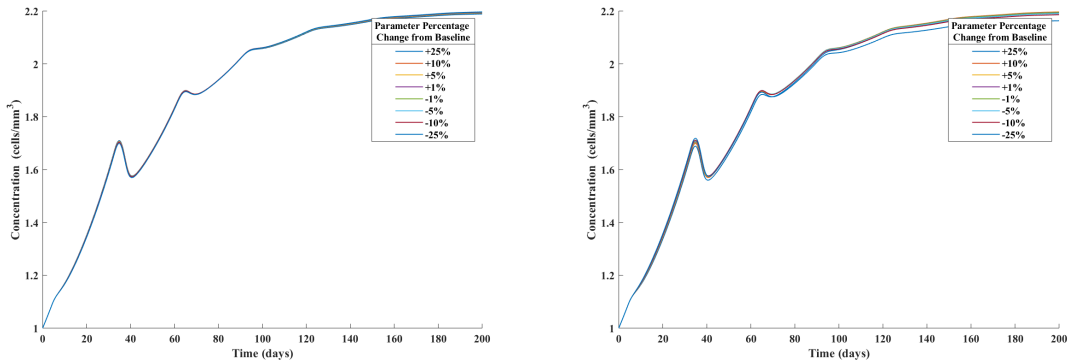

(a) Sensitivity analysis of parameters, k_{BR}

(b) Sensitivity analysis of parameter, q_2

Figure 4.11: Sensitivity analysis of parameters: k_{BR} and q_2. Here, k_{BR} is the rate ate which helper T cells transition into Tregs due to the presence of BCCs and q_2 is the Hill function half maximum value for the increased transition of helper T cells to Tregs. We observe that with large and small perturbations, we still see BCCs entering into a state of dormancy and not many changes to the final breast cancer population.

outcome mimics the expected final result, breast cancer outgrowth. We note that the parameter that has the largest fluctuation from the baseline is $r_B - \delta_B$, which follows from our comment on breast cancer aggression.

When fluctuating the parameters guiding the recruitment of Tregs by BCCs, k_{BR} and q_2, we do not observe major changes from the original results of dormant BCCs (Figure 4.11). We note that our initial breast cancer population size and our growth rate of BCCs is low. When we increase both of these BCC parameters, we see greater fluctuations in the final results when varying our Treg recruitment parameters (see Figure 4.12). This leads us to believe that the recruitment of Tregs is more important when the BCCs are proliferating faster and are in larger quantities.

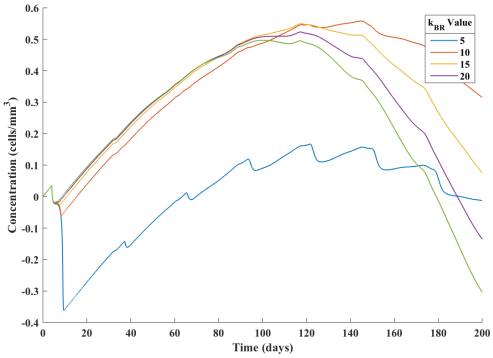

(a) Sensitivity analysis of parameters, k_{BR}

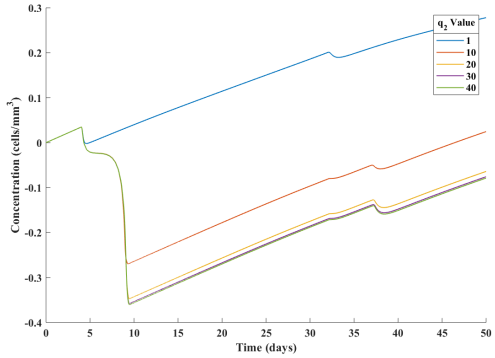

(b) Sensitivity analysis of parameter, q_2

Figure 4.12: Sensitivity analysis of parameters with more aggressive BCCs: k_{BR} and q_2. Here, k_{BR} is the rate ate which helper T cells transition into Tregs due to the presence of BCCs and q_2 is the Hill function half maximum value for the increased transition of helper T cells to Tregs. We observe that with a more aggressive BCC population, we see greater fluctuations in growth and contraction of BCCs. Here we set our initial BCC population to 1K/mm^3, $r_B - \delta_B$ to 0.02, and k_B to 1.

4.4 Discussion

A major drawback of this breast caner dormancy model is in the final scaling of the results. Specifically, in our simulations we observe that the final total amount of breast cancer cells falls into the range of 2 cells/mm^3 of blood. We assert that this result may off by an order of magnitude to be realistic to cells in the body. However, we were able to stimulate the immune system with this small number of breast cancer cells and in general, we expect that experimentally the amount of cells would fall out of the range of clinical measuring capabilities.

Another downfall of this model is that it lacks key details of breast cancer dormancy. While we were able to simulate immune-induced dormancy, true breast cancer dormancy is a complex system including cell cycle arrest, immune evasion, and angiogenic influences, which would require a systems biology approach to fully

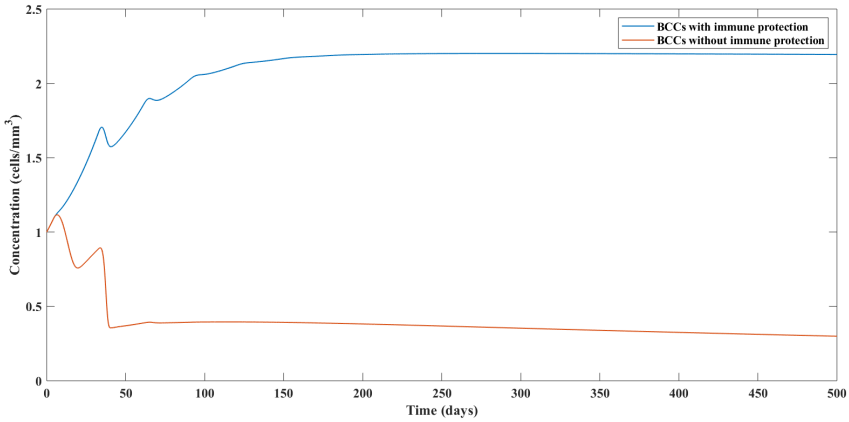

Figure 4.13: BCCs with and without immune protection. We observe that without immune protection, the BCCs fall under a viable threshold for survival following the initial immune response.

quantify. Moreover, we were unable to incorporate the differences in latency periods and dormancy escape. Our model mainly focuses on early stage dormancy and lacks key aspects of chronic disease, such as T cell exhaustion.

When creating this model we aimed to not only display breast cancer cells entering into a state of dormancy, but show that the cause of this dormancy is specific to the disseminated breast cancer cells in the bone marrow. When removing the protective aspects of the breast cancer cells specific to dormancy in the bone marrow, including recruitment of Tregs and CTL function suppression, as seen in Figure 4.13, we see that without the incorporation of immuno-protection, the breast cancer cells cannot survive past the initial immune stimulation.

Breast cancer dormancy, and cancer dormancy in general, involves many factors that are gradually being experimentally accessible. Though we acknowledge that our model is limited in scope in comparison to all of known and unknown factors of dormancy, we were able to capture numerous aspect of the adaptive im-

munity dynamics, ranging from memory T cell activation and contraction to the necessity of regulatory T cells in the survival of dormant breast cancer cells in the bone marrow.

Chapter 5: T Cell Exhaustion

5.1 Overview

One aspect that is common among most chronic diseases in the fact that over time, T cells begin to experience exhaustion. This phenomenon not only reduces the effectiveness and functions of T cells, but as a chronic disease progresses it has the ability to cause T cells to go through apoptosis. As shown in Figure 5.1, the process by which exhaustion occurs happens in a hierarchical manner, starting with a decline in the IL-2 production and ending in apoptosis of T cells. While the stages of exhaustion are better documented for CD8+ T cells, CD4+ T cells are also believed to undergo exhaustion and through cytokine production, play an important role in the overall exhaustion of the adaptive immune system. The cause of T cell exhaustion has been linked to a few mechanisms both intrinsic and extrinsic to the cell, with one of the most well studied being the programmed cell-death protein 1 (PD-1) and its ligand, PD-L1. Through the combination of cell surface inhibitory receptors, cytokines, and regulatory immune cells, immunoregulation is at the center of T cell exhaustion.

In this chapter, we develop a mathematical model to study the dynamics of T cell exhaustion through the lens of immunoregulation. We expand upon the delayed

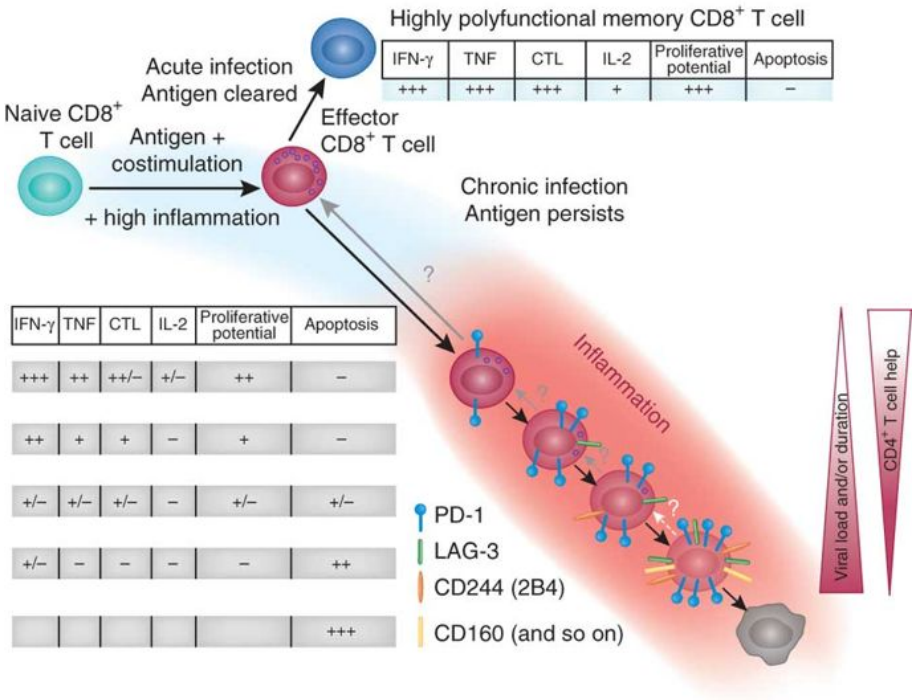

Figure 5.1: Representation of the hierarchical nature of T cell exhaustion. Figure taken from Wherry (2011).

differential equation (DDE) model created in Chapter 3 in order to mimic T cell exhaustion with consistent and continuing antigen stimulation as observed in a chronic infection. It is shown that while early immune responses to antigen stimulation result in dynamics similar to acute infections, as exhaustion increases, the immune cells become less effective and the antigen cells eventually outgrow the system. We conclude that with this model we are able to both mimic exhausted T cell behavior in a hierarchical manner and capture key components of immunoregulatory induced T cell exhaustion.

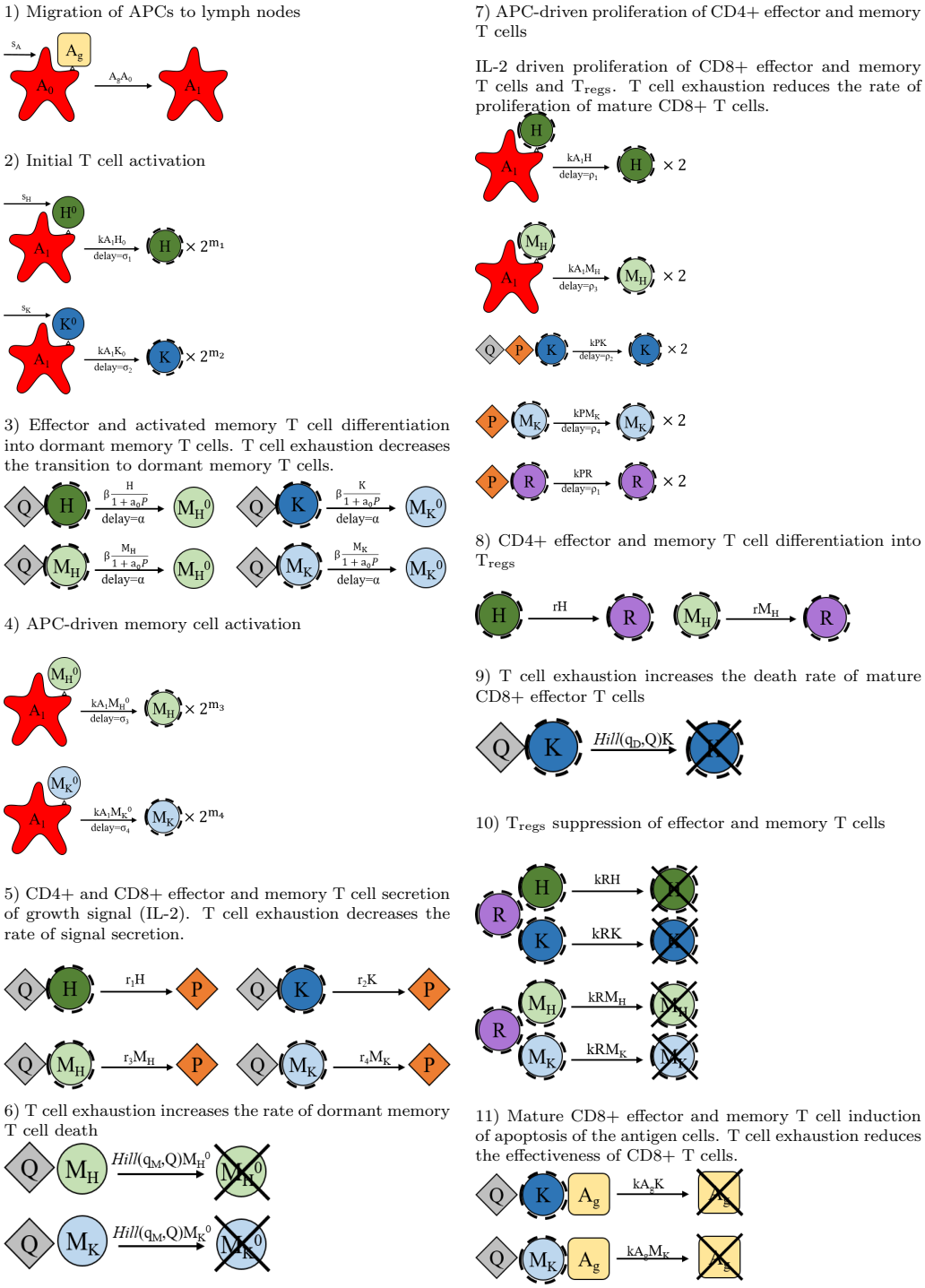

Figure 5.2: Diagram of T cell exhaustion model (5.1)-(5.18). The compartments are represented as follows: A_0: immature APCs, A_1: mature APCs, H^0: naïve helper T cells, H: mature helper T cells, K^0: naïve cytotoxic T cells, K: mature cytotoxic cells, M_H^0: dormant memory helper T cells, M_H: activated memory helper T cells, M_K^0: dormant memory cytotoxic T cells, M_K: activated memory cytotoxic cells, P: IL-2 concentration, R: regulatory T cells, A_g: antigen concentration, and Q: level of T cell exhaustion.

5.2 T Cell Exhaustion Model

Following the framework developed in Chapter 3, we develop a delayed differential equation model which includes a separate compartment for T cell exhaustion. Our model is shown in Figure 5.2, and includes the following elements:

1. Immature APCs, $A_0(t)$, become mature APCs, $A_1(t)$ when they interact with antigen cells, $A_g(t)$. Mature APCs travel to the lymph nodes.

2. In the lymph nodes, the naïve helper T cells, $H^0(t)$, and naïve cytotoxic T cells, $K^0(t)$, interact with the mature APCs and begin to undergo the minimal developmental program. Here the helper T cells and the CTLs divide m_1 and m_2 times, respectively, for the duration of σ_1 and σ_2, respectively.

3. In primary immune response, during the contraction phase, when the amount of mature APCs, $A_1(t)$, is low, mature helper T-cells and mature CTLs, transition into dormant memory helper cells, $M_H^0(t)$, and dormant memory CTLs, $M_K^0(t)$, respectively. In the contraction phase of secondary and subsequent immune responses, mature helper T cells and activated memory helper cells, $M_H(t)$, both transition to $M_H^0(t)$. Similarly, mature CTLs and activated memory CTLs, $M_K(t)$, both transition to $M_K^0(t)$ during the contraction phase of secondary and subsequent immune responses. The duration of the transition into $M_H^0(t)$ and $M_K^0(t)$ is α. As T cell exhaustion increases in the system, the rate at which these cells transition into dormant memory T cells decreases.

4. In secondary and subsequent immune responses, the dormant memory T cells,

interact with mature APCs causing them begin the minimal developmental program. Here the memory helper T cells and the memory CTLs divide m_3 and m_4 times, respectively, for the duration of σ_3 and σ_4, respectively.

5. Both mature effector T cells and activated memory T cells secrete the growth signal IL-2, $P(t)$. T cell exhaustion affects the ability of these cells to secrete IL-2. Specifically, as exhaustion increases, secretion decreases.

6. Increased exhaustion in the system prevents dormant memory T cells from surviving long term and the death rate increases.

7. Once mature T cells and activated memory T cells complete the minimal developmental program, they become effector T cells and continue to divide. The CD4+ cells continue to proliferate in response to an interaction with the mature APCs, while CD8+ cells proliferate in response to stimulation by IL-2. The ability for mature CD8+ T cells to rapidly proliferate is hindered by more T cell exhaustion.

8. A proportion of mature helper T cells and activated memory helper cells transition into regulatory T cells in response to stimulation antigen cells.

9. As T cell exhaustion lasts long term, mature effector CTLs result in increased cell death.

10. Regulatory T cells suppress mature effector T cells as well as activated memory T cells. They also proliferate in response to IL-2 stimulation.

11. Mature CTLs and activated memory CTLs induce apoptosis in antigen cells. The functionality of CTLs is decreased with an increase in T cell exhaustion.

The model for adaptive immunity dynamics with the incorporation of T cell exhaustion is given by the following equations:

$$\dot{A}_0 = s_A - d_0 A_0(t) - A_g(t)A_0(t), \tag{5.1}$$

$$\dot{A}_1 = A_g(t)A_0(t) - d_1 A_1(t), \tag{5.2}$$

$$\dot{H}^0 = s_H - \delta_0 H^0(t) - kA_1(t)H^0(t), \tag{5.3}$$

$$\begin{aligned}\dot{H} &= 2^{m_1} kA(t-\sigma_1)H^0(t-\sigma_1) - kA_1(t)H(t) + 2kA_1(t-\rho_1)H(t-\rho_1) \\ &\quad - (\delta_H + r)H(t) - kR(t)H(t) - \mathfrak{b}(Q)\frac{H(t)}{1+a_0P(t)},\end{aligned} \tag{5.4}$$

$$\dot{K}^0 = s_k - \delta_0 K^0(t) - kA_1(t)K^0(t), \tag{5.5}$$

$$\begin{aligned}\dot{K} &= 2^{m_2} kA_1(t-\sigma_1)K^0(t-\sigma_1) - k(1 - Hill(q_K, Q(t)))K(t)P(t) \\ &\quad + 2k(1 - Hill(q_K, Q(t)))P(t-\rho_2)K(t-\rho_2) - \delta_{KQ} Hill(q_D, Q(t))K(t) \\ &\quad - \delta_K K(t) - k_E R(t)K(t) - \mathfrak{b}(Q)\frac{K(t)}{1+a_0P(t)},\end{aligned} \tag{5.6}$$

$$\begin{aligned}\dot{M}_H^0 &= \mathfrak{b}(Q)\frac{H(t-\alpha)}{1+a_0P(t-\alpha)} + \mathfrak{b}(Q)\frac{M_H(t-\alpha)}{1+a_0P(t-\alpha)} + (r_{MH} - \delta_{MH})M_H^0(t) \\ &\quad - k_{MH}A_1(t)M_H^0(t) - Hill(q_M, Q(t))M_H^0(t)),\end{aligned} \tag{5.7}$$

$$\begin{aligned}\dot{M}_H &= 2^{m_3} k_{MH} A_1(t-\sigma_3)M_H^0(t-\sigma_3) - kA_1(t)M_H(t) + 2kA(t-\rho_1)M_H(t-\rho_1) \\ &\quad - (\delta_H + r)M_H(t) - kR(t)M_H(t) - \mathfrak{b}(Q)\frac{M_H(t)}{1+a_0P(t)},\end{aligned} \tag{5.8}$$

$$\begin{aligned}\dot{M}_K^0 &= \mathfrak{b}(Q)\frac{K(t-\alpha)}{1+a_0P(t-\alpha)} + \mathfrak{b}(Q)\frac{M_K(t-\alpha)}{1+a_0P(t-\alpha)} + (r_{MK} - \delta_{MK})M_K^0(t) \\ &\quad - k_{MK}A_1(t)M_K^0(t) - Hill(q_M, Q(t))M_K^0(t)),\end{aligned} \tag{5.9}$$

$$\dot{M}_K = 2^{m_4} k_{MK} A_1(t-\sigma_4) M_K^0(t-\sigma_4) - kP(t)M_K(t) + 2kP(t-\rho_2)M_K(t-\rho_2)$$
$$- \delta_K M_K(t) - k_E R(t) M_K(t) - \mathfrak{b}(Q)\frac{M_K(t)}{1+a_0 P(t)}, \tag{5.10}$$

$$\dot{P} = \mathfrak{r}_1(Q)H(t) + \mathfrak{r}_2(Q)K(t) + \mathfrak{r}_3(Q)M_H(t) + \mathfrak{r}_4(Q)M_K(t) - \delta_P P(t)$$
$$- kP(t)K(t) - kP(t)R(t) - kP(t)M_K(t), \tag{5.11}$$

$$\dot{R} = r(H(t) + M_H(t)) + 2kP(t-\rho_1)R(t-\rho_1) - kP(t)R(t) - \delta_H R(t), \tag{5.12}$$

$$\dot{A}_g = a(t) + [(r_A - \delta_A)A_g(t) - k_A(1 - Hill(q_A, Q(t)))A_g(t)K(t)$$
$$- k_A A_g(t) M_K(t)] \times \theta(A_g(t) - 10^{-18}). \tag{5.13}$$

$$\dot{Q} = r_Q Hill(q_Q, A_1(t)) - \delta_Q Q(t) \tag{5.14}$$

where,

$$Hill(q, Q(t)) = \frac{Q^3(t)}{q^3 + Q^3(t)}, \tag{5.15}$$

$$\mathfrak{b}(Q) = \beta \times (1 - Hill(q_M, Q(t))), \tag{5.16}$$

$$\mathfrak{r}_*(Q) = r_* \times (1 - Hill(q_R, Q(t))), \tag{5.17}$$

$$q_R < q_K < q_M < q_A < q_D. \tag{5.18}$$

A_0 represents the concentration of immature APCs at the site of infection, while A_1 is the concentration of mature APCs that are presenting antigen in the lymph nodes. H^0 represents the concentration of naïve helper T cells and H is the concentration of mature helper T cells. Similarly, K^0 and K represent the concentration of immature and mature cytotoxic T cells, respectively. M_H^0 and M_H represent the concentration

of dormant and activated memory helper T cells, while M_K^0 and M_K represent the concentration of dormant and activated memory cytotoxic T cells. Finally, P represents IL-2 concentration, R represents regulatory T cell concentration, A_g represents antigen concentration, and Q represents the amount of T cell exhaustion.

Equation (5.1) describes the immature APCs that are available in the body to respond to antigen stimulation. We assume is a constant supply rate of the cells, s_A, and a death rate, d_0, that is proportionate to the amount of immature APCs. Immature APCs are stimulated by the antigen in the system, A_g, and through this stimulation immature APCs become the mature APCs in the lymph nodes described by (5.2). Mature APCs also have a death rate proportional to the amount of mature APCs in the system, d_1.

Equations (5.3) and (5.5) describe naïve T cell populations for helper T cells and cytotoxic T cells, respectively. Both populations have constant supply rates, s_H and s_K, and a death rate, δ_0, that is proportional to the amount of each of the naïve T cell populations. These naïve T cells transition into their respective effector T cell populations based on the mass action interaction with mature APCs.

The mature helper T cell population is described by Equation (5.4). After the naïve CD4+ cells are activated by mature APCs, the first term shows the rate at which they enter the minimal developmental program where they undergo m_1 cell divisions. The amount of time required for this developmental program is characterized by the time delay σ_1. Once the cells are fully mature, CD4+ cells are further stimulated by APCs and proliferate, the rate at which this division occurs is shown by the second and third terms. The amount of time required for a mature helper T

cells to divide is represented by the time delay ρ_1.

Mature helper T cells are removed from the system by either natural cell death, δ_H, differentiation into regulatory T cells, r, regulatory T cells suppression, or differentiation into dormant memory cells. Since we assume that dormant memory cells are formed during the contraction phase of immune response, the last term shows the rate of CD4+ cells switching to dormant memory cells occurring when the amount of mature APCs is low. The rate at which cells transition to dormant memory CD4+ T cells depends on the amount of exhaustion in the system—the more exhaustion in system, the less cells that transition to memory T cells.

Equation (5.6) describes the mature cytotoxic T cell population. Similar to the mature helper T cells, the first term shows the rate at which naïve CD8+ cells enter the mature cell population after undergoing the minimal developmental program of m_2 cell divisions. The amount of time required for this developmental is given by the time delay of ρ_2. Further proliferation of CD8+ cells is activated by IL-2, the second and third terms, with the duration of one cell division of CD8+ cells shown corresponding to the time delay ρ_2. The rate at which cells proliferate is impacted by the amount of exhaustion in the system. If more exhaustion is present in the system, the rate at which CTLs proliferate decreases.

CD8+ cells exit the system by either cell death, suppression by regulatory T cells, or by differentiating into dormant memory CTLs when the amount of IL-2 is low, or during the contraction phase. The death of CD8+ cells depends not just on natural cell, δ_K, death but also on the amount of exhaustion, δ_{KQ}. When there is more exhaustion present, the rate at which these T cells are removed increases.

Similar to CD4+ T cells, when more exhaustion is present in the system, less CD8+ T cells will transition to the dormant memory T cell compartment.

Equations (5.7) and (5.9) describe the dormant helper and CTL memory cells, respectively. The first two terms of each equation show the rates at which cells are transitioning from either their respective mature T cell populations or their respective activated memory T cell compartment. We assume that after transition from the effector T cell compartments, dormant memory T cells can be activated only after a time α passes. The third term describes the proportionate growth rate, r_{M*}, and natural death rate, δ_{M*}. The next term describes the rates at which dormant cells become activated. Similar to naïve T cells, dormant memory cells become activated based on the mass action interaction with mature APCs. Finally, there is an additional death term with a rate that is proportional to the amount of exhaustion in the system.

The activated memory T cell populations are described by Equations (5.8) and (5.10), representing CD4+ and CD8+ T cells, respectively. Similar to the activation of non-memory T cells, after the dormant memory cells become activated by mature APCs, the first term shows the rate at which they enter the minimal developmental program where they undergo m_3 and m_4 cell divisions. The amount of time required for this developmental program is characterized by the time delays σ_3 and σ_4. Once cells are fully activated, CD4+ cells are further stimulated by APCs and proliferate, while CD8+ cells are further stimulated by IL-2. The amount of time required for activated memory CD4+ and CD8+ T cells to divide is represented by the time delays ρ_1 and ρ_2, respectively.

Activated memory CD4+ T cells are removed from the system by either natural cell death, δ_H, differentiation into regulatory T cells, r, regulatory T cells suppression, or differentiation into dormant memory cells. Similarly, activated memory CD8+ T cells are removed from the system either through natural cell death, δ_K, regulatory T cells suppression, or differentiation into dormant memory cells. Since we assume that dormant memory cells are formed during the contraction phase of the immune response, the last term of both equations corresponds to the rate of activated memory cells switching to dormant memory cells occurring when the amount of mature IL-2 is low. Just as with non-memory T cells, with greater exhaustion in the system, we will have a lower rate of transition to dormant memory T cells.

Equation (5.11) describes the amount of IL-2 in the system. The first four terms show the rate at which IL-2 is secreted by mature helper t cells ($\mathfrak{r}_1$), mature CTLs ($\mathfrak{r}_2$), activated memory helper T cells ($\mathfrak{r}_3$), and activated memory CTLs ($\mathfrak{r}_4$). The amount of exhaustion in the system also impacts the amount of IL-2 that is secreted by the cells, with more exhaustion causing less IL-2 secretion. The cytokine has a decay rate, δ_P, proportionate to its amount. IL-2 is also consumed by mature CTLs, activated memory CTLs, and Tregs, given by the last three terms.

The dynamics of regulatory T cells is governed by equation (5.12). The first term gives the rate at which mature helper T cells and activated memory T cells differentiate into Tregs. The next two terms describe the rate at which Tregs further proliferate based on IL-2 activation, with the duration of one Treg cells division characterized by the time delay ρ_1. Tregs exit the system by the same natural death rate of helper T cells, δ_H.

Equation (5.13) describes the dynamics of antigens. The first term describes their proportionate growth rate, r_A, and death rate, δ_A. Antigens are removed from the system via interaction with mature CTLs and activated memory CTLs, the second and third term, respectively. The rate at which non-memory CTLs remove antigen from the system is affected by the amount of exhaustion present, with more exhaustion leading to a lower rate of removal. $\theta(t)$ is the Heaviside equation, with

$$\theta(t) = \begin{cases} 0 & t < 0, \\ \frac{1}{2} & t = 0, \\ 1 & t > 0. \end{cases}$$

Here, the Heaviside equation prevents the antigen compartment from changing once its population falls below a threshold which we set as 10^{-18} K/mm^3. Consequently, this addition reduces the amount of consistent stimulation of the immune cells in the model. Finally, the last term, $a(t)$, describes the source of antigens, which is used to induce secondary immune response during simulation of the model.

The final equations of our system, (5.14)-(5.18), represent the amount of exhaustion in the system and how it affects the system's dynamics. In Equation (5.14), exhaustion is added to the system proportional to the amount of mature APCs at the rate, r_Q, and decays at a rate δ_Q. Equation (5.15) characterizes the Hill equation used to determine the affect of exhaustion on the different cell compartments. Equation (5.16) represents how the rate of transition to dormant memory T cells, β, is affected by exhaustion, while Equation (5.17) represents the change in IL-2 secre-

tion by exhaustion. Depending on the hierarchical order in which T cell exhaustion affects T cell functioning, we order the terms q_* to characterize when the amount of exhaustion in the system will effect the individual functionality, from varying, q_R, to more exhaustion, q_D.(5.18)

5.3 Numerical Results

Using the values found in Table 5.1, we numerically solve Equations (5.1)-(5.14). All simulations are carried out using the MATLAB solver DDESD. The assumptions that are made for these simulations are as follows:

1. Memory T cells are naturally slow growing and slowly dying; specifically, they proliferate and go through natural cell death at the same rate. However, with T cell exhaustion, these cells have an increased death rate.

2. Even if there is sign of antigen clearance, we assume there is consistent antigen growth, such as in DNA based chronic diseases.

3. All antigen stimulations are of the same magnitude and are equally spaced in time. Moreover, in order to induce consecutive antigen stimulations every 40 days, we set the function $a(t)$ in our antigen compartment to the following:

$$a(t) = \begin{cases} 2 & 40i \leq t \leq 40i + 1, i = 0, 1, 2, ... \\ 0 & otherwise. \end{cases}$$

The number 40 is arbitrary, but we choose to pick a time frame that is greater

Parameter	Description	Estimate	Source
$A_0(0)$	Initial concentration of immature APCs	10	Kim
$H_0(0)$	Initial concentration of naïve CD4+ T cells	0.06	Kim
$K_0(0)$	Initial concentration of naïve CD8+ T cells	0.04	Kim
s_A	Supply rate of immature APCs	0.3	Kim
d_0	Death rate of immature APCs	0.03	Kim
d_1	Death rate of mature APCs	0.8	Kim
s_H, s_K	Supply rate of naïve CD4+ and CD8+ T cells, respectively.	0.0018, 0.0012	Wilson
k	Kinetic coefficient	5	Wilson
δ_0	Death rate of naïve T cells	0.03	Wilson
δ_H, δ_K	Natural death rate of mature CD4+ and CD8+ T cells, respectively.	0.23, 0.4	Wilson
δ_{KQ}	Death rate of CD8+ T cells due to T cell exhaustion	3	estimated
m_1, m_2	Number of divisions in the minimal developmental program for naïve CD4+ and CD8+ T cells, respectively.	2, 7	Wilson
σ_1, σ_2	Duration of the minimal developmental program for naïve CD4+ and CD8+ T cells, respectively.	1.46, 4	Wilson
ρ_H, ρ_K	Duration of one T cell division for mature CD4+ and CD8+ T cells, respectively	11/24, 1/3	Wilson
k_E	Kinetic coefficient for CTL-Treg interactions	20	Wilson
β	Rate of differentiation of mature effector T cells into dormant memory effector T cells	0.3	estimated
α	Duration of time for cells to switch into dormant memory effector T cells	20	estimated
r_{MH}, r_{MK}	Growth rate of dormant memory CD4+ and CD8+ T cells, respectively.	0, 0	assumed
δ_{MH}, δ_{MK}	Death rate of dormant memory CD4+ and CD8+ T cells, respectively.	0, 0	assumed
k_{MH}, k_{MK}	Kinetic coefficient for mature APC-memory T cell interactions	5, 5	estimated
m_3, m_4	Number of divisions in the minimal developmental program for dormant memory CD4+ and CD8+ T cells, respectively.	3, 8	estimated
σ_3, σ_4	Duration of the minimal developmental program for dormant memory CD4+ and CD8+ T cells, respectively.	1, 3	estimated
a_0	Magnitude of dependence of dormant memory T cell differentiation on IL-2	5	estimated
r_1, r_2	Rate of IL-2 secretion by mature CD4+ and CD8+ T cells, respectively	10, 1	Kim
r_3, r_4	Rate of IL-2 secretion by activated memory CD4+ and CD8+ T cells, respectively	12.3, 3.3	estimated
δ_P	Decay rate of free IL-2	5.5	Wilson
r	Rate of differentiation of mature and activated memory CD4+ T cells into regulatory T cells	10	estimated
r_A	Growth rate of antigen cells	1	estimated
δ_A	Death rate of antigen cells	0.4	estimated
k_A	Kinetic coefficient for CTL-antigen interactions	2	estimated
r_Q	Growth rate of T cell exhaustion	0.5	estimated
δ_Q	Decay rate of T cell exhaustion	0.007	estimated
q_R, q_K, q_M, q_A, q_D, q_Q	Hill function half maximum points	5, 6, 7, 8, 9, 0.44	estimated

Table 5.1: Estimates of parameters for model (5.1)-(5.18). All concentrations are measured in K/mm^3 and time is in days. Initial conditions not provided in the table are zero.

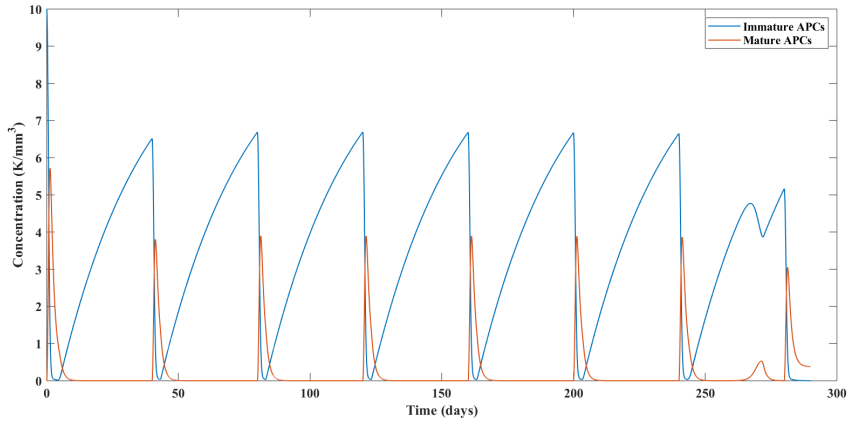

Figure 5.3: The dynamics of immature and mature APCs. While the level of exhaustion is low, we see a repetitive behavior for activation of APCs. When the amount of exhaustion reaches a high enough level, around day 275, we see APC behavior shift to coincide with increased the antigen load.

than the transition time for dormant memory T cells.

In Figure 5.3, we observe the dynamics of the both immature and mature APCs. Throughout the first seven immune stimulations, we see dynamics that is consistent with acute infections. Once the exhaustion reaches a high enough level, between the seventh and eighth stimulations, we notice a decrease in the immature APCs. This is due to the transition into mature APCs in response to the increase population of antigen cells growing. Once the antigen compartment outgrows the system, the mature APCs remain at around 1 K/mm^3.

The level of exhaustion is shown in Figure 5.4. This concentration grows every time there is an increase in the amount of mature APCs, i.e., whenever we stimulate the immune system with more antigen. Exhaustion decays whenever there is a decrease in the amount of mature APCs, but it does not go to zero before the next antigen stimulation. This lack of full decay results in the amount of exhaustion continuously accumulating over time until the antigen compartment outgrows the

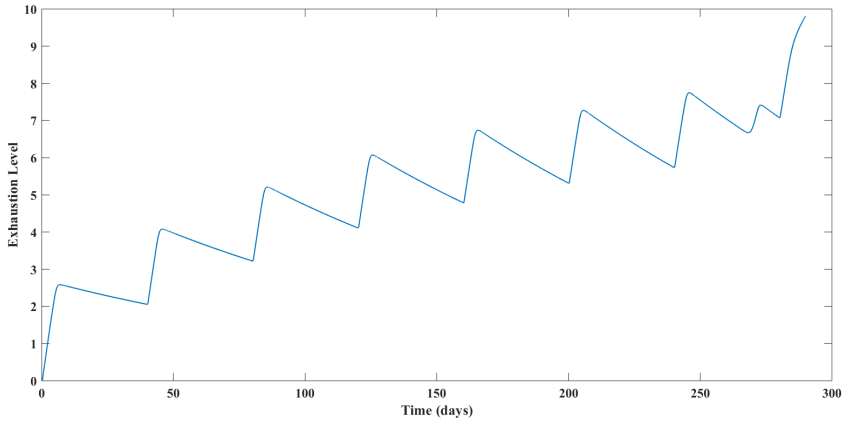

Figure 5.4: The dynamics of the level of T cell exhaustion. The amount of exhaustion increases whenever we see an increase in the amount of mature APCs and decays slowly when the amount of mature APCs is low. Once the antigen cells outgrow the system at around dy 280, we see high levels of exhaustion with no reduction.

system around 285 days, which results in consistently growing exhaustion.

In Figure 5.5 we see the dynamics of the mature non-memory T cells. The first three immune stimulations mimic the primary and subsequent immune responses similar to that in acute infections, where the primary response is significantly smaller in the subsequent responses. This is due to the fact that in acute infections, we have activated memory T cells that are the primary effector T cells in secondary and subsequent immune responses. However, as the exhaustion level rises, we begin to see an increase in the amount of non-memory T cells at play following antigen stimulation. This increase remains in place until the level of exhaustion is high enough to cause elimination of effector T cells, around 275 days.

The dynamics of dormant memory T cells is shown in Figure 5.6. We observe that even though dormant memory cells are created 25 days after an immune response, due to exhaustion, these cells are not maintained in the long term. As the level of exhaustion increases, the rate at which these dormant memory cells decay

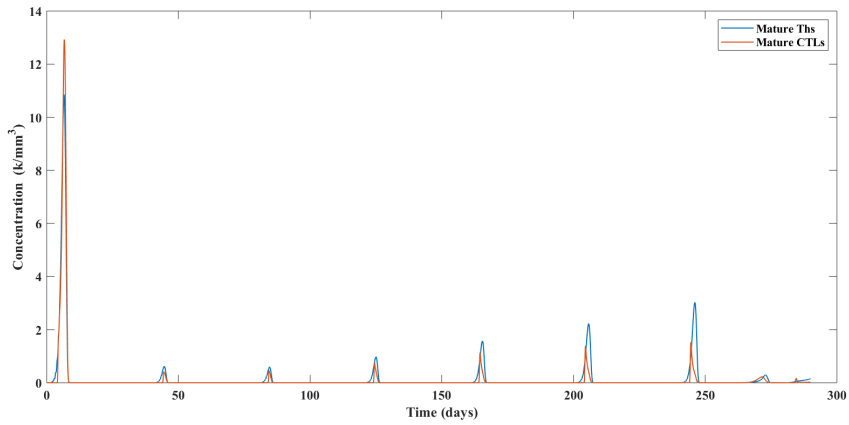

Figure 5.5: The dynamics of mature Ths and CTLs. With low T cell exhaustion, following the primary response, we see little to no effector T cells. As exhaustion advances, we see an increase in the amount of effector T cells until around 275 days, where due to the high amount of T cell exhaustion causes a decrease in the amount of effector T cells.

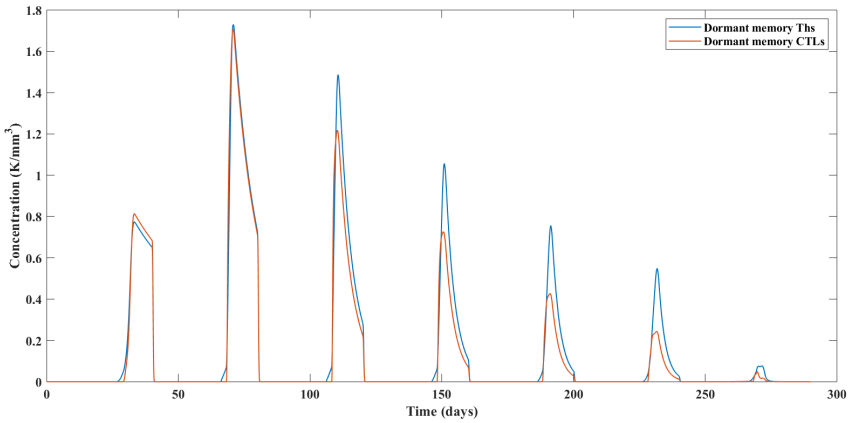

Figure 5.6: The dynamics of dormant memory T cells. As the amount of T cell exhaustion increases, the ability for dormant memory T cells to exists long term decreases eventually resulting with little contribution of memory T cells in subsequent immune responses.

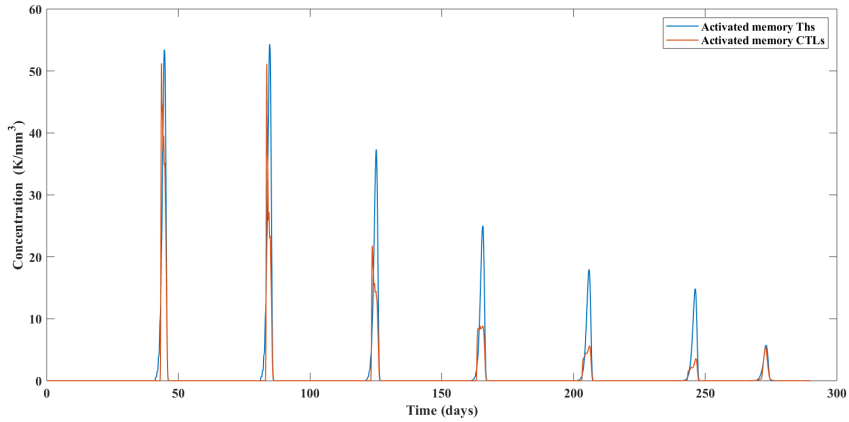

Figure 5.7: The dynamics of activated memory T cells. Due to the reduction of dormant memory T cells, we see a gradual decrease in the amount of activated memory T cells as the amount of T cell exhaustion increases.

increases. This lack of dormant memory T cells over time affects the amount of activated memory cells that are present during an immune response (see Figure 5.7). Similar to non-memory T cells, the activated memory T cells perform as they would during an acute infection in the second and third immune stimulation, while the level of exhaustion is low. As the level of exhaustion increases, we see the amount of activated memory T cells decrease as a result of fewer dormant memory T cells. By the time of the last immune stimulation at 280 days, the high level of exhaustion causes the dormant memory T cells to deplete to the point where activated memory T cells are not even present.

The amount of IL-2 and Treg concentration is shown in Figure 5.8. We observe that after the third antigen stimulation, the level of IL-2 remains at very low levels, consistent with the fact that reduction in IL-2 production requires the lowest amount of exhaustion. The amount of Tregs present is proportional to the amount of effector T cells, with the first three stimulations mimicking the behavior seen in

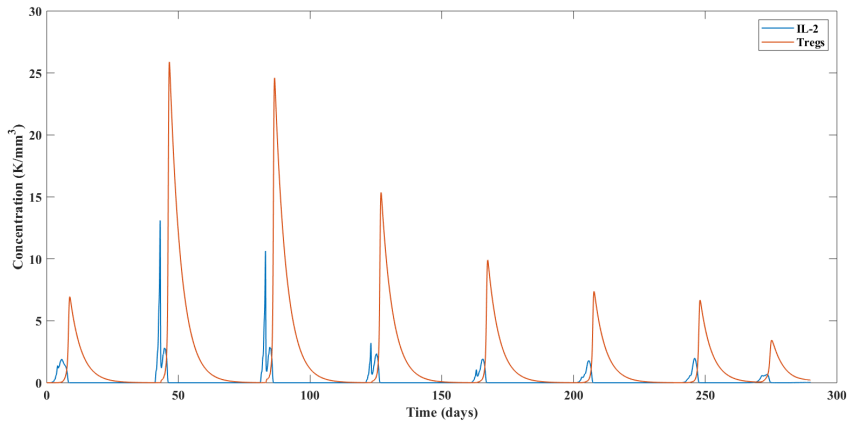

Figure 5.8: The dynamics of IL-2 and Tregs. The amount of IL-2 secreted as well as the amount of Tregs that are present mimic the amount and type of T cells that are activated. From primary to secondary response there is a 6 fold increase in the amount of both concentrations. As T cell exhaustion increases, we see a gradual decrease in both concentrations in subsequent immune responses.

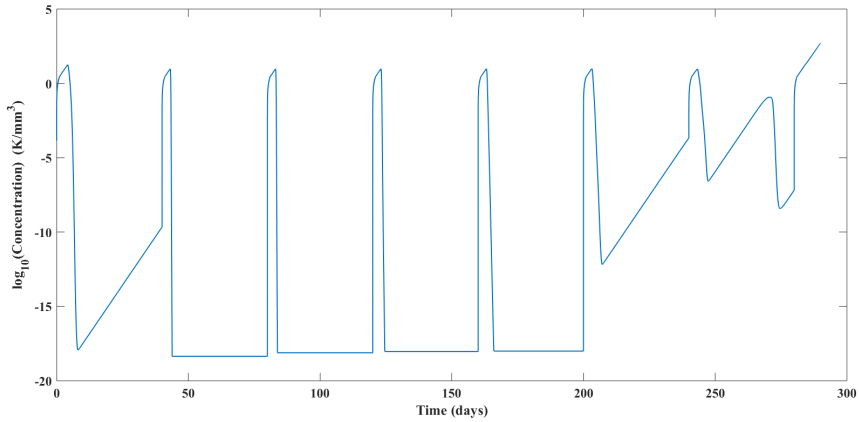

Figure 5.9: The dynamics of antigen concentration. With antigen stimulation occurring every 40 days, we see the equivalent of antigen clearance within the first six responses when T cell exhaustion is low. As the amount of T cell exhaustion increases, we observe a reduced clearance in antigen concentration until it is no longer cleared which happens around day 280.

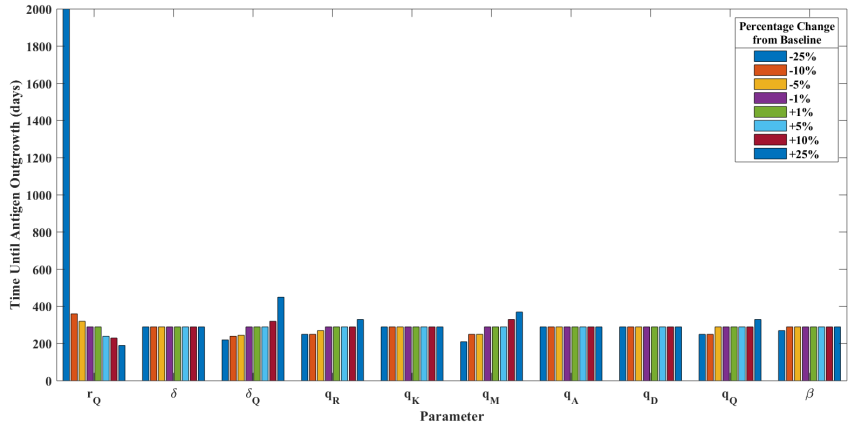

Figure 5.10: Sensitivity analysis of T cell exhaustion parameters. All of the exhaustion parameters are varied to determine which has the greatest impact on the time until the immune cells are no longer able to control the antigen compartment. About half of the parameters do not affect the final outgrowth time. The parameters which cause more fluctuations in time include, exhaustion growth and decay rates, r_Q and δ_Q, and the half maximum values for IL-2 production, q_R, memory T cell decay, q_M, and exhaustion growth, q_Q.

acute infections and the remaining stimulations resulting in a gradual decrease in Tregs.

The dynamics of the final compartment, antigen concentration, are displayed in Figure 5.9. The first five stimulations of the antigen compartment mimic acute infections, where for the most part the antigen gets eliminated by the immune system cells. Following the sixth stimulation, we begin to witness the weakening of the immune response with the antigen compartment not fully being eliminated and continuously growing. By the time we stimulate the immune response for the seventh time, the antigen compartment is able to continuously grow and eventually outgrow the system, at around 285 days.

5.3.1 Parameter Analysis

We performed sensitivity analysis on the T cell exhaustion parameter values found in Table 5.1. Using these parameters as the baseline, we calculated the amount of time required for the antigen compartment to overtake the immune system for values ranging $\pm 25\%$ of the baseline parameters (Figure 5.10). While around half of the exhaustion parameters are robust, we observe that the most sensitive parameters are the exhaustion growth and decay rates, r_Q and δ_Q, as well as the half maximum values for IL-2 production, q_R, memory T cell decay, q_M, and exhaustion growth, q_Q.

Given that the level of exhaustion at any given time depends on the values of r_Q, δ_Q, and q_Q we expect that these three parameters would result with large fluctuations in the amount of time required for the antigen compartment to outgrow. In conjunction, the rate at which IL-2 is produced and the rate at which dormant memory T cells decay both play integral roles in the overall effectiveness of an immune response. This is especially true given that in our system IL-2 is responsible for the proliferation of CD8+ T cells. Moreover, considering that exhaustion causes CD8+ T cells to lose their effector function, when there is a depletion of dormant memory T cells, the system loses its capacity to fight infection, a function that is traditionally held by memory T cells in acute infections.

5.4 Discussion

While this model does a good job of mimicking the behavior of adaptive immune cells during T cell exhaustion, there are several drawbacks our approach. Since we manually stimulate the antigen compartment, we lose the ability to have an antigen that continuously evolves with the immune cells in the system. This way of modeling antigen works well for chronic diseases that are associated with a constant supply of antigen from an external source, such as in chronic viral infections. It is not a good way of modeling T cell exhaustion when the supply of antigen cells comes from a source intrinsic to the system, such as with continuously replicating cancer cells.

Our model has the capacity to further elaborate on the different pathways in which exhaustion occurs. This added detail could potentially allow for the simulation of therapies specific to the pathway, such as PD-1 blockade therapy.

There are two main aspects of our approach that stand out for further investigations. First, our model suggests that being able to quantify the rate at which exhaustion accumulates and delays allows for better understanding of long term prognosis of a disease. Second, given the importance of memory T cells to our system, our results suggest that further investigations into the way in which memory T cells are impacted by T cell exhaustion would also be beneficial. Initially, we set out to create a model with the ability to better understand the dynamics of immune cells during chronic infections and how these cells are impacted by exhaustion over time. We demonstrated the ability to capture the hierarchical nature of T cell exhaustion

as well as the long term effects of uncontrolled exhaustion, antigen outgrowth. With further detail for specific antigens, we posit the notion that our model can be used to further investigate long term effects and therapies for different antigen types.

Chapter 6: Conclusions

There are many directions that we could pursue with our mathematical models. Below we outline two potential routes: a simplified acute infection model, and a model extension to breast cancer dormancy escape.

6.1 A Simplified Acute Infection Model

While we were able to achieve the desired dynamics in the model found of Chapter 3, due to the considerable amount of detail, we lose the ability to conduct extensive analysis. Moreover, with the parameter analysis that was conducted, we see that even with large fluctuations in the majority of parameters, there is no significant change in the final result. This leads us to consider creating a simplified model opens the door for mathematical analysis, while maintaining the primary features of the full model.

A preliminary attempt of the simplification of our acute infection model is found below:

$$\dot{K}^0 = s_k - \delta_0 K^0(t) - kA_g(t)K^0(t), \tag{6.1}$$

$$\dot{K} = 2^{m_1} kA_g(t-\sigma_1)K^0(t-\sigma_1) + 2^{m_2} k_M A_g(t-\sigma_2)M(t-\sigma_2) - (\delta_K + r)K(t)$$

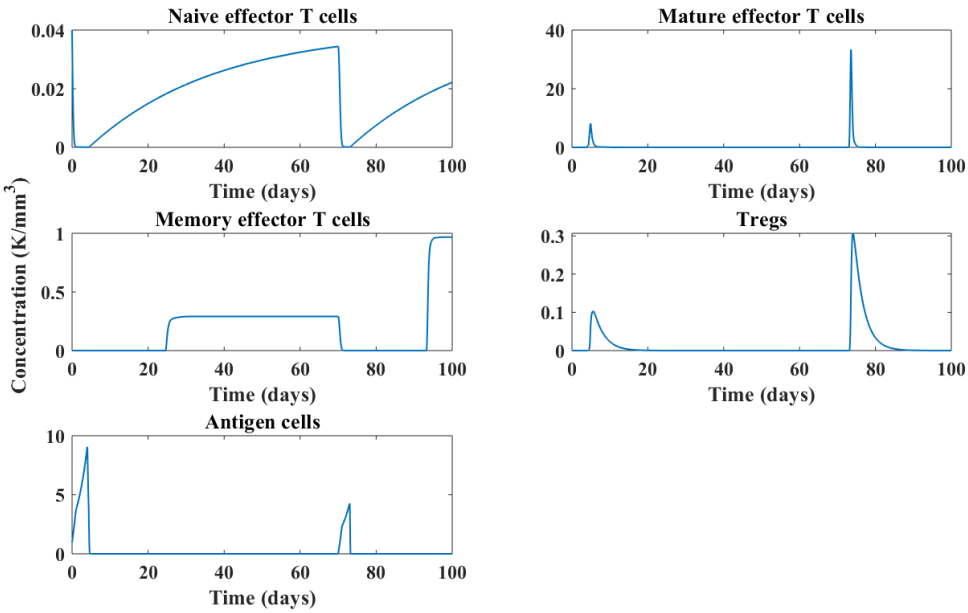

Figure 6.1: Preliminary simulations of simplified acute infection model 6.1-6.5. Memory cells are created and remain steadily at low levels—around 5-10%—and the secondary immune response is quicker and of greater magnitude.

$$- kA_g(t)K(t) + 2kA_g(t-\rho)K(t-\rho) - k_E R(t)K(t) - \beta\frac{K(t)}{1+a_0A_g(t)}, \quad (6.2)$$

$$\dot{M} = \beta\frac{K(t-\alpha)}{1+a_0A_g(t-\alpha)} + (r_M - \delta_M)M_K(t) - k_M A_g(t)M_K(t), \quad (6.3)$$

$$\dot{R} = rK(t) + 2kA_g(t-\rho)R(t-\rho) - ka_g(t)R(t) - \delta_K R(t), \quad (6.4)$$

$$\dot{A}_g = [(r_A - \delta_A)A_g(t) - k_A A_g(t)K(t)] \times \theta(A_g(t) - 10^{-18}) + a(t). \quad (6.5)$$

Here, K^0 and K represent our naive and mature effector T cell concentrations, respectively. M is memory T cells, R represents our regulatory T cells, and A_g is our antigen concentration. Though we lose detail in this simplified model, such as removing IL-2 concentration and removing the separation of activated memory cells and effector T cells, we still maintain key results. Preliminary simulations are shown in Figure 6.1. Similar to the full model, we see an increase in the secondary effector

cells with 5-10% of the total cell population becoming dormant memory T cells. We also see a faster and greater secondary immune response. Since this model has less parameters, a more rigorous analysis of the model and the parameter space may be possible.

6.2 Cancer Dormancy Escape

The body of scientific knowledge of cancer dormancy escape is an ever changing field. We know that the combination of specific cancer type and individual patient factors leads to different secondary tumor sites and a range latency periods before a possible relapse. There have been many theories as to how relapse occurs. While we primarily studied immune-induced dormancy, as mentioned in Chapter 1, cancer dormancy also occurs in combination with cellular dormancy and angiogenesis.

Understanding that all three types of cancer dormancy are happening at the same time gives insight into the numerous ways that may lead to dormancy escape. Regardless of the type, we identify both cell-intrinsic and cell-extrinsic causes to dormancy escape. For cellular-dormancy, we see cell-extrinsic factors leading to cell-intrinsic changes. For example, there is evidence that chronic inflammation can lead to the evolution and mutation of dormant cells, with these cells evolving to escape and cause distant secondary tumor sites. In contrast, in immune-induced dormancy escape, we see the causes being associated with tumor antigen loss, increases in myeloid-derived suppressor cells or Tregs, and even increases in PD-L1 expression, leading to T cell exhaustion [45].

As discussed in Chapters 4 and 5, a good extension of the two chronic infection models produced would be to combine our T cell exhaustion and the breast cancer dormancy models. By doing so, we can gain insight into an antigen specific, chronic infection model that has T cell exhaustion developed as a result of user-independent antigen stimulation. A combined model, will allow us to study how exhaustion plays a role in late stage breast cancer dormancy. This full model would also allow us to test the causes for differences in the latency periods between different breast cancer types.

There are more ways to extend our work to better study cancer dormancy. For instance, we solely model immune-induced dormancy, but experimentally, we see both cellular and immune-induced dormancy. While incorporating cell cycle arrest into our model would result in examining both low and high level views of cancer cells, this systems biology approach to dormancy models would allow for a more complete biological scope.

6.3 Discussion

Mathematical contributions to the study of both acute and chronic infections are constantly evolving to match the details and ever changing nature of experiments. There still is a long way before reaching a good understanding of the immune system during these infections. This work began by asking questions about cancer dormancy and the mathematical contributions to this field of study. However, after learning more on the topic, narrowing down on the complexity surrounding

dormancy, led us to realize that we should first better understand simpler immunological systems, such as the immune response during an acute infection. Moreover, knowing that our aim was to look at a specific chronic infection, we needed to better understand the role of memory in the system. Specifically, we wanted to better understand the mechanisms driving memory cells, their connection to later immune responses, and how exhaustion affects them.

To study these questions, we developed three mathematical models allowing us to gain further insight into memory T cells. In our first model, we aimed to better understand the importance of memory T cells in a secondary immune response. Though initially used to study acute infections, this model became a framework to extend upon for our second and third models. In our second model, we extended the scope of our previous antigen compartment to study breast cancer dormancy in the bone marrow. Here we were able to show the importance of the bone marrow niche for the survival of breast cancer cells. Finally, our last model was created to better understand the effects of T cell exhaustion during chronic infections.

A major component that is missing from our work is a look into how therapies play a role in the dynamics of infections. While there is an extensive set of mathematical contributions studying vaccinations for acute infections and cancer therapies, there are not a lot of studies into T cell exhaustion therapies. There have been, however, recent developments into different exhaustion therapies in cancer, viruses, and other infections, and with our exhaustion model, we have created a framework that can be used to study such therapies.

This dissertation was created with the help of collaboration of both mathe-

maticians and experimentalists. If we were to add clinicians and patient data to the fold, the possibilities are endless in the knowledge that can be gained. While the direction of our initial inquiry into dormancy shifted to fill in the gaps in the mathematical knowledge, I was able to better understand the immunological concepts necessary to create useful mathematical models. More so than finding concrete answers, this project has guided me to better understand the compounding nature of immunological questioning and how one small question can open the door to many.

Bibliography

[1] A Abbas, AH Lichtman, and S Pillai. *Basic immunology : functions and disorders of the immune system*. Elsevier/Saunders, Philadelphia, PA, 2014.

[2] PR Rogers, C Dubey, and SL Swain. Qualitative changes accompany memory t cell generation: faster, more effective responses at lower doses of antigen. *J Immunol*, 164:2338–2346, 2000.

[3] ND Pennock, JT White, EW Cross, EE Cheney, BA Tamburini, and RM Kedl. T cell responses: naive to memory and everything in between. *Adv Physiol Educ*, 37:273–283, 2013.

[4] MK MacLeod, JW Kappler, and P Marrack. Memory cd4+ t cells: generation, reactivation and re-assignment. *Immunology*, 130:10–15, 2010.

[5] M Berard and DF. Tough. Qualitative differences between nave and memory t cells. *Immunology*, 106:127–138, 2002.

[6] B Youngblood, JS Hale, HT Kissick, and et al. Effector cd8 t cells dedifferentiate into long-lived memory cells. *Nature*, 552:404–409, 2017.

[7] D Masopust, V Vezys, AL Marzo, and L Lefrançois. Preferential localization of effector memory cells in nonlymphoid tissue. *Science*, 291:2413–2417, 2001.

[8] V Golubovskaya and L Wu. Different subsets of t cells, memory, effector functions, and car-t immunotherapy. *Cancers*, 8:36, 2016.

[9] C Eichelberger, S Bauchiero, D Point, BMW Richter, GA Prince, and R Schuman. Distinct cellular immune responses following primary and secondary influenza virus challenge in cotton rats. *Cell Immunol*, 243:67–74, 2006.

[10] RS Akondy, M Fitch, S Edupuganti, and et al. Origin and differentiation of human memory cd8 t cells after vaccination. *Nature*, 552:362–367, 2017.

[11] DC Macallan, JAM Borghans, and B Asquith. Human t cell memory: a dynamic view. *Vaccines*, 5:1–12, 2017.

[12] SM Kaech and W Cui. Transcriptional control of effector and memory cd8+ t cell differentiation. *Nat Rev Immunol*, 12:749–761, 2012.

[13] C Gerlach, JW Heijst, E Swart, D Sie, N Armstrong, RM Kerkhoven, D Zehn, MJ Bevan, K Schepers, and TNM Schumacher. One naive t cell, multiple fates in cd8+ t cell differentiation. *J of Exp Med*, 207:1235–1246, 2010.

[14] R. Gomis and S. Gawrzak. Tumor cell dormancy. *Molecular Oncology*, 11:62–78, 2017.

[15] R. Schreiber, L. Old, and M. Smyth. Cancer immunoediting: Integrating immunity's roles in cancer suppression and promotion. *Science*, 331:1565–1570, 2011.

[16] A. Law, E. Lim, C. Ormandy, and D. Gallego-Ortega. The innate and adaptive infiltrating immune systems as targets for breast cancer immunotherapy. *Indocrine-Related Cancer*, 24:R123–R144, 2017.

[17] J. Dittmer. Mechanisms governing metastatic dormancy in breast cancer. *Seminars in Cancer Biology*, 44:72–82, 2017.

[18] N. Walker, J. Patel, J. Munoz, M. Hu, K. Guiro, G. Sinha, and P. Rameshwar. The bone marrow niche in support of breast cancer dormancy. *Cancer Letters*, 380:263–271, 2016.

[19] J. Wherry. T cell exhaustion. *Nature Immunology*, 12:492–499, 2011.

[20] PS Kim, D Levy, and PP Lee. Modeling and simulation of the immune system as a self-regulating network. *Methods Enzymol*, 467:79–109, 2009.

[21] PS Kim, PP Lee, and D Levy. Emergent group dynamics governed by regulatory cells produce a robust primary t cell response. *Bull Math Biol*, 72:611–644, 2009.

[22] PS Kim, PP Lee, and D Levy. A theory of immunodominance and adaptive regulation. *Bull Math Biol*, 73:1645–1665, 2010.

[23] R Eftimie, JJ Gillard, and DA Cantrell. Mathematical models for immunology: current state of the art and future research directions. *Bull Math Biol*, 78:2091–2134, 2016.

[24] K. Wilkie. A review of mathematical models of cancer-immune interactions in the context of tumor dormancy. *Advances in Experimental Medicine and Biology*, 734:201–234, 2013.

[25] D. Coombs, O. Dushek, and PA. van der Merwe. A review of mathematical models for t cell receptor triggering and antigen discrimination. *Mathematical models and immune cell biology*, pages 25–45, 2011.

[26] K. Ganeshan and A. Chawla. Metabolic regulation of immune responses. *Annual Review of Immunology*, 4:322–335, 2014.

[27] D. Barua, W. Hlavacek, and T. Lipniacki. A computational model for early events in b cell antigen receptor signaling: analysis of the roles of lyn and fyn. *Journal of Immunology*, 189:646–658, 2012.

[28] C Gerlach, J Rohr, L Perie, NV Rooij, JV Heijst, A Velds, J Urbanus, S Naik, H Jacobs, J Beltman, RD Boer, and T Schumacher. Heterogeneous differentiation patterns of individual cd8+ t cells. *Science*, 340:635–639, 2013.

[29] J Beltman, A Marée, and R de Boer. Analysing immune cell migration. *Nat Rev Immunol*, 9:789–798, 2009.

[30] C Macnamara and R Eftimie. Memory versus effector immune responses in oncolytic virotherapies. *J Theor Biol*, 377:1–9, 2015.

[31] P Ankomah and B Levin. Exploring the collaboration between antibiotics and the immune response in the treatment of acute, self-limiting infections. *E Proc Natl Acad Sci*, 111:8331–8338, 2014.

[32] F Crauste, E Terry, I Mercier, and et al. Predicting pathogen-specific cd8 t cell immune response from a modelling approach. *J Theor Biol*, 374:66–82, 2015.

[33] Q. Yang, F. Berthiaume F, and IP Androulakis. A quantitative model of thermal injury-induced acute inflammation. *Mathematical Bioscience*, 229:135–148, 2010.

[34] R. Eftimie, J. Bramson, and D. Earn. Interactions between the immune system and cancer: A brief review of non-spatial mathematical models. *Bulletin in Mathematical Biology*, 73:2–32, 2011.

[35] S Michelson and JT Leith. Dormancy, regression, and recurrence: towards a unifying theory of tumor growth control. *Journal of Theoretical Biology*, 169:327–338, 1994.

[36] KM Page and JW Uhr. Mathematical models of cancer dormancy. *Leukemia and Lymphoma*, 46:313–327, 2005.

[37] V. Kuznetsov. Mathematical modeling of the development of dormant tumors and immune stimulation of their growth. *Cybern. Syst. Anal.*, 23:556–564, 1988.

[38] D Wodarz, P Klenerman, and MA Nowak. Dynamics of cytotoxic t-lymphocyte exhaustion. *Proceedings Biological Sciences*, 265:191–203, 1998.

[39] PL Johnson and BF Kochin et al. Vaccination alters the balance between protective immunity, exhaustion, escape, and death in chronic infections. *Journal of virology*, 85:5565–5570, 2011.

[40] S Wilson and D Levy. Functional switching and stability of regulatory t cells. *Bulletin of Mathematical Biology*, 75:1891–1911, 2013.

[41] S Sakaguchi, T Yamaguchi, T Nomura, and M Ono. Regulatory t cells and immune tolerance. *Cell*, 133:775–787, 2008.

[42] S Sakaguchi. Conditional stability of t cells. *Nature*, 468:41–42, 2010.

[43] JK Flynn, GT Belz, JD Altman, R Ahmed, DL Woodland, and PC Doherty. Virus-specific cd8+ t cells in primary and secondary influenza pneumonia. *Immunity*, 8:683 – 691, 1998.

[44] WL Lu, L Jansen, and WJ Post et al. Impact on survival of early detection of isolated breast recurrences after the primary treatment for breast cancer: a meta-analysis. *Breast Cancer Res Treat*, 114:403, 2009.

[45] MH Manjili. Tumor dormancy and relapse: From a natural byproduct of evolution to a disease state. *Cancer Research*, 77:2564–2569, 2017.